

Interactive comment on “Investigation of hydrological time series using copulas for detecting catchment characteristics and anthropogenic impacts” by

T. Sugimoto, A. Bárdossy, G. S. S. Pegram and J. Cullmann

Point-to-Point Response to Editor’s review – *referee comments in italics*

This manuscript has now undergone a second review by one of the original reviewers. This reviewer indicated that they are satisfied with the manuscript and feel that the manuscript can move forward with publication. Both reviewers point out that the novelty of the manuscript is appropriate for HESS and I concur that the use of copula asymmetry is a promising approach to addressing the complex question of attribution of observed catchment behavior. I have carefully read the manuscript and have comments that I feel must be addressed before the manuscript can be accepted. I consider these comments minor because they are not technically substantive but they still must be addressed completely for this manuscript to be accepted. I have only listed examples in the specific comments below and I ask the authors to carefully review the manuscript to address these comments fully.

The authors must review the HESS guidelines to ensure that the manuscript is in compliance with established requirements for notation, figures, text and equations. See: http://www.hydrology-and-earth-system-sciences.net/for_authors/manuscript_preparation.html

1. Notation:

- There are a few instances that I caught where the guidelines are not followed such as 'k' in lines 98 and 137.

Author’s Response (HESS Guideline) – “*HESS guideline with double quotation*”

Thank you very much for giving thoughtful remarks and fair critics which is important for the completion of this research work. It turned out that many notations in the manuscript do not conform to the HESS guideline, which must have been checked and improved during minor or major revision.

The HESS Guideline was thoroughly checked and the corresponding parts in the manuscript were revised reflecting the regulations. The following are the examples of HESS guideline and how the manuscript was corrected:

“Multi-letter variables, if they cannot be avoided, should be roman”

→ The variables like $Var(t)$ should be $Var(t)$

“Textual subscripts or superscripts should not be italic (e.g. x_{max} , T_{min} where "max" and "min" stand for maximum and minimum, respectively).” → The variables like $Var_{cop}(c_1, c_2)$ should be $Var_{cop}(c_1, c_2)$

“Single-letter variables or parameters and user-defined function symbols should be italic (e.g. x , Y , β , $f(x)$)”

→ All the variable like k for time lag should be italic

“Equations: They should be referred to by the abbreviation ‘Eq.’”, “The abbreviation ‘Fig.’ should be used when it appears in running text” → The reference to the equation or figure should not be “equation (10)” or “Figure 10”, but should be “Eq. (10)” or “Fig. 10”.

“Quotations can also be used to denote an unfamiliar or newly coined term or phrase. They may also be used to introduce a term but only once at the first instance” → For the first use of terms “asymmetry1” and “asymmetry2”, double quotation should be used.

- The use of long variable names is confusing to the reader. Especially the terms asymmetry1 and asymmetry2 when you also have notation for A1 and A2. This is quite confusing to the reader. Also, sometimes asymmetry1 and asymmetry2 are italicized and other times not. A thorough editing of the manuscript is needed to ensure consistency in notation and clarity.

Author's Response (The usage of the term “asymmetry”):

We acknowledge very important point was raised by the reviewer for this article. This is also related to the issue that the manuscript completely follows the HESS Guideline, but the following points also should have been clarified:

- asymmetry1 and asymmetry2 are terms to describe asymmetric characteristic of data, but functions.
- $A_1(k)$ and $A_2(k)$ are functions to evaluate the asymmetric characteristic of data

Then “asymmetry2” should be always roman and the term like “minimum of asymmetry2” should have been avoided, because asymmetry2 is neither a function nor a variable. The usage “asymmetry2” as a term seems still sensible in some context to explain the asymmetric characteristic of data. The asymmetry1 and asymmetry2 are related to different characteristic of discharge or catchment in general, $A_1(k)$ and $A_2(k)$ are one of the way to capture them, while anonymous referre#1 suggested alternative approach that they can be modeled with advanced asymmetry function (Serfling and Xiao, 2007). For the revising the text, it was carefully thought out that how they should be expressed and the expression “minimum of asymmetry2” were all deleted. The definition of asymmetry $A_1(k)$ and $A_2(k)$ are revised as follow:

(revised text for definition of asymmetry)

The two types of asymmetry, “asymmetry1” and “asymmetry2”, are considered for two diagonals on 2-dimensional copulas, which can be captured as a function of time lag k (Li, 2010):

$$A_1(k) = E[(U_t - 0.5)(U_{t+k} - 0.5)((U_t - 0.5) + (U_{t+k} - 0.5))] \quad (1)$$

$$= \int_0^1 \int_0^1 (u_t - 0.5)(u_{t+k} - 0.5)(u_t + u_{t+k} - 1)c(u_t, u_{t+k}) du_t du_{t+k}$$

$$A_2(k) = E[-(U_t - 0.5)(U_{t+k} - 0.5)((U_t - 0.5) - (U_{t+k} - 0.5))] \quad (2)$$

$$= \int_0^1 \int_0^1 -(u_t - 0.5)(u_{t+k} - 0.5)(u_t - u_{t+k})c(u_t, u_{t+k}) du_t du_{t+k}$$

where $u_t = F_Z(z(t))$, $u_{t+k} = F_Z(z(t+k))$. $A_1(k)$ and $A_2(k)$ are asymmetry functions corresponding to asymmetry1 and asymmetry2 respectively.

2. *Figures: The figure captions and figures should be stand-alone. Abbreviations are used and not explained. One cannot view the figures and understand what is being shown by reading the captions. All figures need to be modified to comply with this. As examples, I point to the following:*

- *Figure 1: The full site names are shown here but then abbreviations are used in later figures. You need to show both the full name and abbreviation in Figure 1 for the reader to make the connection with what is shown in Figures 4, 5, etc.*

- *Figure 2: There is no label on the contour colors. What is being plotted?*

Author's Response (Caption and Abbreviation of the figures):

As it was mention by editor, it is clearly written in HESS Guideline as “the abbreviations used in the figure must be defined, unless they are common abbreviations or have already been defined in the text.”. Now, the proper abbreviations are added to Figure1 and Figure 12 next to the full name of discharge gauging stations and precipitation measuring stations. The caption of Figure 2 is modified and the labels for the contour colors are added so that it will be more comprehensive.

3. *Some details are missing:*

- *In line 181, are the times series normalized according to Grimaldi, 2004?*

Author's Response (Grimaldi's Method):

Yes and sorry for the ambiguity. The line 181 was slightly modified as follow.

(original text) Adopting this method, all the time series are normalized in this study.

(revised text) Adopting Grimaldi's method, all the time series are normalized in this study.

- *What is meant in line 170 that the "rate of increase and decrease of discharge are not symmetric"?*

Author's Response (possible better explanation for line 170): Thank you for pointing out the imperfect expression which is important for this research work. This is related to the mechanism why $A_2(k)$ get negative for discharge data and it might be well illustrated in Fig.3. So, the original text was modified based on this notion as follow :

(original text) rates of increase and decrease of discharge are not symmetric

(revised text) the rates of increase and decrease of discharge are not symmetrical in the upper limb compared to the lower limb of the hydrograph (Fig. 3)

- *line 235, the "minimum" of what?*

Author's Response: It refers to the minimum of temperature and discharge, which should have been clearly denoted and original text was slightly modified.

(original text) the standard deviation and the minimum in a time window centered on time t defined by

(revised text) the standard deviation and the minimum of discharge and temperature in a time window centered on time t defined by

4. *The abstract fails to mention the most important aspect of copula asymmetry in the context of this paper - that it can be used to attribute catchment behavior. I would remove some details about the two measures of the copula domain in the abstract and add 1-2 sentences about application of these new measures to hydrology.*

Author's Response (Abstract):

We agree that it is very important to mention that the asymmetry can be used to the catchment behavior. The abstract in the manuscript was edited, reflecting this notion.

References

Li, J., 2010. Application of copulas as a new geostatistical tool 1–161.

Serfling, R., Xiao, P., 2007. A contribution to multivariate L-moments: L-comoment matrices. J. Multivar. Anal. 98, 1765–1781. doi:10.1016/j.jmva.2007.01.008

Investigation of hydrological time series using copulas for detecting catchment characteristics and anthropogenic impacts

Takayuki Sugimoto¹, András Bárdossy^{1,2}, Geoffrey G. S. Pegram² and Johannes Cullmann³

¹ Institute for Modelling Hydraulic and Environmental Systems, University of Stuttgart, Stuttgart, Germany

² Civil Engineering Program, University of KwaZulu-Natal, Durban, South Africa

³ Water & Climate Department, World Meteorological Organization, Geneva, Switzerland

Abstract. Global climate change can have impacts on characteristics of rainfall-runoff events and subsequently on the hydrological regime. Meanwhile, the catchment itself changes due to anthropogenic influences. However, it is not easy to prove the link between the hydrology and the forcings. In this context, it might be meaningful to detect the temporal changes of catchments independent from climate change by investigating existing long term discharge records. For this ~~purpose, a new stochastic system based on copulas for time series analysis is introduced. While widely used time series models are based on linear combinations of correlations assuming a Gaussian behavior of variables, a~~

A statistical tool like the copula has the advantage to scrutinize the dependence structure of the data ~~and, thus, can be used to attribute the catchment behavior by focusing on the following aspects of the statistics defined in the copula domain: (1) Copula asymmetry, which can capture the non symmetric property of discharge data, differs from one catchment to another due to the intrinsic nature of both runoff and catchment. (2) Copula distances can assist in identifying catchment change by revealing the variability and interdependency of dependence structures. in the uniform domain independent of the marginal. Two measures in the copula domain are introduced herein:~~

~~1. Copula asymmetry is defined for copulas and calculated for discharges; this measure describes the non-symmetric property of the dependence structure and differs from one catchment to another due to the intrinsic nature of both runoff and catchment.~~

~~2. Copula distance is defined as Cramér von Mises type distance calculated between two copula densities of different time scales. This measure describes the variability and interdependency of dependence structures similar to variance and covariance, which can assist in identifying the catchment changes.~~

These measures are calculated for 100 years of daily discharges for the Rhine rivers ~~and tributaries.~~ and these analyses detected epochs of change in the flow sequences. ~~Comparing~~ In a follow-up study, we compared the results of copula asymmetry and copula distance applied to two flow models: between an (i) Antecedent Precipitation Index (API) and (ii) simulated discharge time series by a hydrological model. The results of copula based analysis of hydrological time series seem to support the assumption that the Neckar catchment had started to change around 1976 and stayed unusual until 1990. ~~we show the interesting signals of systematic modifications along the Rhine rivers in the last 30 years.~~

Keywords : Catchment discharge characteristics, Copula stochastic analysis, API, Model uncertainty

1. Introduction

In order to understand the water cycle behavior of a region, it is important to determine its characteristics, but this is difficult to achieve due to the diversity of the system response at different time and space scales. In particular, temporal variability makes parameter estimation difficult and the assessment of model

47 uncertainty essential. As a part of the endeavor to understand the hydrological system, the objective of this
48 research, assessing the anthropogenic impacts on the catchment characteristic independent of the climate
49 change, is therefore important, yet hard to accomplish.

50 | —The first possible approach is to statistically test the existence or change of trend in hydrological time
51 series which can be related to climate changes or anthropogenic impacts. Mann-Kendall's Test was
52 performed to confirm the existence of a trend in the annual discharge, precipitation and sediment loads,
53 then the human intervention and climate impacts based on the available information of the catchments
54 were discussed (Wu et al., 2012). Pettitt's Method (Pettitt, 1979) can be used to detect the time point of
55 trend alternation and analyze the impacts based on a double mass curve (Gao et al., 2012) or a
56 hydrological model (Karlsson et al., 2014). These non-parametric methods for detecting the signal seem,
57 however, not capable enough of explaining when and how much the system had changed, thus making it
58 still difficult to relate the change due to human activities.

59 | —On the other hand, runoff events are initiated by precipitation then modified by the state and physical
60 features of the catchment. This implies that the integrated information of catchment status might be
61 retrieved by analyzing the discharge time series itself. Focusing on this property, the attempts can be made
62 for capturing the temporal dependence structure of runoff by time series models. The classical time series
63 model, autoregressive integrated moving average (ARIMA), is designed to describe a stationary stochastic
64 process based on the temporal correlation structure of Gaussian random variables (Box and Jenkins, 1976).
65 However, the stationarity of the data is not guaranteed in reality, thus a number of alternative approaches
66 have been suggested. While the application of Fourier analysis is basically for stationary process, the
67 analysis using empirical mode decomposition (Huang et al., 1998) overcomes the restriction of stationarity
68 by allowing the frequency and local variance of a time series to vary within a component and to separate
69 the signals adaptively by scale. Autoregressive Conditional Heteroskedasticity (ARCH) models lose the
70 assumption of stationarity to a certain extent so that variance is not constant, however models the variance
71 in a similar way to ARIMA. Although inventions and efforts to overcome the limitation of stationarity

72 have been made, it seems still inadequate to model dynamic changes of hydrological processes with these
73 time series models.

74 Alternatively there is a statistical concept, the copula, which has advantages to model the multivariate
75 dependence independently from marginals and recently adopted in the field of hydrology. A Copula (Sklar,
76 1959) is a multivariate probability distribution designed to flexibly model dependence structure in the
77 uniform (quantile) domain. The use of copulas in hydrology can be found for the assessment of extreme
78 events by considering flooding as a joint behavior of peak and volume (De Michele and Salvadori, 2003).
79 Copulas have been applied to describe the spatio-temporal uncertainty of precipitation (Bárdossy and
80 Pegram, 2009) or the inhomogeneity of groundwater parameters (Bárdossy and Li, 2008). Asymmetry of
81 dependence in a time series can be tested in the framework of a finite state Markov chain's transition
82 probability matrix (Sharifdoost et al., 2009). Dissimilarity measures can be defined by means of a copula
83 modelling the correlation structure of pairs of discharge time series in order to identify the similarity of
84 catchments with the purpose of transferring catchment properties from one to the other (Samaniego et al.,
85 2010). We aim at utilizing copulas as an alternative to classical time series models and an efficient tool for
86 time series analysis to overcome these hydrological challenges.

87 The main interest of this study is to assess the human intervention and climate change impacts on
88 hydrological regime for the strategy of future development in the region. For achieving this goal, 7 daily
89 discharge gauging stations in South-West Germany (Fig. [ure](#) 1), which have 100 years daily discharge
90 records, were chosen and extensively analyzed. The gauging stations Andernach, Kaub, Worms and
91 Maxau are located in the main stream of the Rhine, while Kalkofen, Cochem and Plochingen are located
92 on tributaries. For further analysis, daily precipitation and temperature records in the Baden-Württemberg
93 state of Germany for the last 50 years were obtained from the German Weather Service. Also, 77 discharge
94 records obtained from the Global Runoff Data Centre in Germany were utilized.

95 The following are the novel aspects introduced in this study: (1) The catchment characteristics are defined
96 based on copulas and estimated from discharge data. Also the changes of catchment characteristics are

97 investigated by tracing the temporal change of these statistics. (2) A method to model systematic changes
 98 of dependence structure with the help of copulas is suggested, then its variability and interrelationship with
 99 the time series are examined. (3) Anthropogenic impacts are assessed by the discharge - precipitation
 100 relation using API and a hydrological model with copula based measures.

101 This article is divided into five sections. After the introduction, the basic methodology for applying
 102 copulas to discharge time series is introduced in the second section. Thirdly, the measures of asymmetry in
 103 copulas are defined and estimated for the discharges of the [R-river Rhine](#) and other catchments. The
 104 determination of the temporal change of the asymmetry of the copulas is treated in the third section as well.
 105 In the fourth section two topics are treated: (i) the analysis based on copula distances for the observed
 106 discharges and (ii) the comparison of observed discharge with API (Antecedent Precipitation Index) time
 107 series and simulated discharge time series with a hydrological model. The conclusion is given in the fifth
 108 section.

109 2. Methodology

110 In this section, the application of copulas to time series is articulated after a brief introduction. The very
 111 basics about copulas are presented here ; further information can be obtained from (Joe, 1997) or (Nelsen,
 112 2006).

113 2.1 Basic Methodology

114 In probability theory and statistics, a copula is a multivariate probability distribution for which the
 115 marginal probability distribution of each variable is uniform.

$$116 \quad C : [0,1]^n \rightarrow [0,1] \quad (1)$$

$$117 \quad C(\mathbf{u}^{(i)}) = u_i \quad \text{if } \mathbf{u}^{(i)} = (1, \dots, 1, u_i, 1, \dots, 1) \quad (2)$$

118 Any multivariate distribution can be described by a copula and its marginal distributions as was proven by
 119 Sklar's theorem (Sklar, 1959):

Field Code Changed

Field Code Changed

120

$$F(\mathbf{x}) = C(F_{X_1}(x_1), \dots, F_{X_n}(x_n)) \quad (3)$$

Field Code Changed

121

where $F_{X_i}(x_i)$ represents the i -th marginal distribution of a multivariate random variable \mathbf{X} . The copula

122

density can be derived by taking partial derivatives of the copula:

123

$$c(u_1, \dots, u_n) = \frac{\partial^n C(u_1, \dots, u_n)}{\partial u_1 \dots \partial u_n} \quad (4)$$

Field Code Changed

124

The advantage of using copulas is that the marginal is detached from the multivariate distribution and

125

the dependence structure can be examined in the uniform compact domain for different types of data.

126

2.2 Basic Hypothesis of Temporal Copulas

127

For the application of copulas to time series analysis, a stochastic system should be presumed to be

128

similar to the case of spatial copulas (Bárdossy and Li, 2008): the random variable at time t is described as

129

$Z(t)$ and in general there may exist non-Gaussian dependency among the elements of $Z(t)$. Then

130

stationarity is defined for each subset of times $t_1, \dots, t_n \subset N$ and time lag k such that

131

$\{t_1 + k, \dots, t_n + k\} \subset N$ and for each set of possible values z_1, \dots, z_n :

132

$$\begin{aligned} P(Z(t_1) < z_1, \dots, Z(t_n) < z_n) = \\ P(Z(t_1 + k) < z_1, \dots, Z(t_n + k) < z_n) \end{aligned} \quad (5)$$

Field Code Changed

133

For the given random function $Z(t)$, a set $S(k)$ containing pairs of ranked values is defined as a

134

function of time lag k as follows:

135

$$S(k) = \{(F_z(z(t))), (F_z(z(t+k)))\} \quad (6)$$

Field Code Changed

136

Thus, a 2-dimentional autocopula for stochastic time series is a function of time lag k for the set $S(k)$

137

similar to the case of spatial copula (Bárdossy and Li, 2008):

138

$$C_i(k, u_1, u_2) = P[F_z(Z(t)) < u_1, F_z(Z(t+k)) < u_2] \quad (7)$$

Field Code Changed

139 where $(u_1, u_2) \in S(k)$. Thus, a 2-dimensional empirical copula density can be constructed based on
 140 conditional empirical frequencies on a regular $g \times g$ grid and kernel density smoothing (Bárdossy, 2006):

$$141 \quad c^* \left(\frac{2i-1}{2g}, \frac{2j-1}{2g} \right) = \frac{g^2}{|S(k)|} \cdot \left| \left\{ (u_1, u_2) \in S(k); \frac{i-1}{g} < u_1 < \frac{i}{g} \text{ and } \frac{j-1}{g} < u_2 < \frac{j}{g} \right\} \right| \quad (8)$$

142 where $|S(k)|$ denotes the cardinality (the number of elements in a set) of set $S(k)$.

143 3. Copula Asymmetry in Discharge Time Series

144 High and low values might have different dependences in general. Measuring the asymmetry of copulas
 145 could reveal substantial aspects of time series data, which are not illuminated in the Gaussian approach.
 146 Statistics defined on copula shape and calculated from observed discharge time series we believe to be a
 147 new idea. The two types of Asymmetry, “asymmetry1” and “asymmetry2”, are can be considered
 148 functions are defined for two diagonals on 2-dimensional copulas, which can be described as a
 149 function of time lag k (Li, 2010):

150 Asymmetry1 and Asymmetry2 are defined as:

$$151 \quad A_1(k) = E[(U_t - 0.5)(U_{t+k} - 0.5)((U_t - 0.5) + (U_{t+k} - 0.5))] \\ = \int_0^1 \int_0^1 (u_t - 0.5)(u_{t+k} - 0.5)(u_t + u_{t+k} - 1)c(u_t, u_{t+k}) du_t du_{t+k} \quad (9)$$

$$152 \quad A_2(k) = E[-(U_t - 0.5)(U_{t+k} - 0.5)((U_t - 0.5) - (U_{t+k} - 0.5))] \\ = \int_0^1 \int_0^1 -(u_t - 0.5)(u_{t+k} - 0.5)(u_t - u_{t+k})c(u_t, u_{t+k}) du_t du_{t+k} \quad (10)$$

153 where $u_t = F_Z(z(t))$, $u_{t+k} = F_Z(z(t+k))$. $A_1(k)$ and $A_2(k)$ are asymmetry functions corresponding to
 154 asymmetry1 and asymmetry2 respectively. Figure 2 shows an idealization of the asymmetries between a
 155 pair of variables $U(t)$ and $U(t+k)$, showing that the tails of the distributions have a large impact on
 156 each type of asymmetry. The measure of asymmetry compares the dependency between low and high
 157 values and quantifies how much it is not symmetric. For example, in a 2-dimensional copula, $A_1(k)$ is

Field Code Changed

Formatted: Font: Italic

Field Code Changed

Field Code Changed

Formatted: Lowered by 5 pt

positive if the probability density is higher in the upper right corner than in the lower left corner. On the contrary, $A_1(k)$ is negative if the probability density is higher in the lower left corner. $A_2(k)$ is the asymmetry for the other diagonal of a 2-dimensional copula.

Figure 3 shows the scatterplot of ranked values of a discharge time series with time lag $k = 1$ as a sample of an empirical autocopula and its relation with storm hydrographs. This figure displays (i) where each pair of values on a hydrograph can be plotted on an empirical copula, demonstrating that (ii) the dependence structure is not symmetric especially for $A_2(k)$.

This illustration provides the insight that asymmetry can be related to the shape of a unit hydrograph as well as the notion that asymmetry might be used for advanced modeling of hydrological time series.

3.1 Asymmetry and catchment characteristics

Asymmetry [functions](#) can be considered as statistics calculated from the observed discharge time series and an important assumption can be made: “asymmetry2-is related to catchment characteristics”. This idea will be discussed and demonstrated in this section. Figure 5 (upper left) shows parts of the hydrographs of 7 gauging stations in southwest Germany.

First, an important natural property of discharge seen in this figure is that the durations of high flow and low flow periods are not symmetric: Flood events, which are initiated by rainfall or snowmelt, do not continue for a long time because the duration of runoff to rivers is comparatively short. On the other hand, discharge keeps decreasing and stays low for no rain periods. This means that, if two consecutive values in a time series are chosen for small time lag k ([day](#)), these two values are likely to be less correlated for high values but more correlated for low values, which leads to negative value of $A_1(k)$.

This implies that the intrinsic temporal distribution of precipitation can be investigated based on this asymmetry, possibly with advanced asymmetry functions such as bivariate moments based on L-moments (Brahimi et al., 2015).

Second, the rates of increase and decrease of discharge are not symmetrical in the upper limb compared to the lower limb of the hydrograph (Fig. 3): Soon after the rainfall, the river flow rises sharply, but - Once the rain stops and peak discharge is observed, then the water level starts to decrease, typically more slowly on the recession than the rising limb of the hydrograph. This, which leads to the negative values of $A_2(k)$ for small time lags k (day) and the notion that - This asymmetry can be related to the shape of the hydrograph, and therefore the characteristics of the runoff and catchment. In addition, it can be said the annual cycle in Fig. 4Fig. 4 is not symmetric in the same sense a hydrograph is not symmetric.

The change of $A_2(k)$ with time lag k [days] is now discussed. The point is that these statistics for small time lags k can be more related to the catchment and rainfall characteristics of the region, while asymmetry for larger time lags k can capture the inter-seasonal characteristic of the climate in the region.

In order to reduce such seasonal impacts on the analysis of hydrological time series, deseasonalization measures can be applied, for example, for daily stream flow (Grimaldi, 2004). Adopting Grimaldi's this method, all the time series are normalized in this study. First, the mean μ_i on the i -th calendar day is

calculated as the expectation of the random variable X_i . Then, the annual cycle of the mean μ_i^* (Fig. 4Fig. 4 left) is calculated as a smoothed version of μ_i by linearly weighting the neighboring values along i and summing them up. The smoothed annual cycle of standard deviations σ_i^* (Fig. 4Fig. 4 right) can be obtained in the same way. Then the normalized time series is defined by dividing the original time series $Z(t)$ by σ_i^* after subtracting μ_i^* as follows

$$\underline{Z_{norm}(t)} = \frac{Z(t) - \mu_{t|365}^*}{\sigma_{t|365}^*} \quad \underline{Z_{nom}(t)} = \frac{Z(t) - \mu_{t|365}^*}{\sigma_{t|365}^*} \quad (11)$$

where $t|365$ is $t \pmod{365}$ and represents calendar day at time t [day]. Figure 5 (upper right) shows parts of normalized discharge time series from the 7 gauging stations. It should be noted that the process still appears to be non-Gaussian after this transformation and the seasonality for small time lags k might not have been fully eliminated. Figure 5 (bottom left and bottom right) shows the variation of asymmetry

Formatted: Font: Italic

Formatted: Font: Not Bold

Formatted: Font: Not Bold

Field Code Changed

Formatted: Font: Not Bold

Formatted: Font: Not Bold

Formatted: Font: Not Bold

Formatted: Font: Not Bold

Field Code Changed

functions for 7 discharge time series corresponding to time lag k , similar to correlograms, in addition to the confidence interval of Gaussian process.

The confidence intervals in the figures are gained by calculating $A_2(k)$ for 100 realizations of stationary Gaussian process which are fitted to the observed discharge of Andernach. The result shows that the process is clearly different from Gaussian and the influence of asymmetry is significantly large.

It can be seen that the variation of $A_2(k)$ of discharge without normalization (Figure 5 bottom left) has a larger impact of seasonality for bigger k ($k > 40$), while its impacts are mitigated after the normalization (Figure 5 bottom right). Furthermore, as a consequence of normalization, a sharp drop down of $A_2(k)$ for small time lags k emerged which might be regarded as a catchment indicator. Therefore, the selected/critical properties for small time lags k is formulated by (i) taking the minimum value of $A_2(k)$ for the time lag $k < 50$ and (ii) the lag k at the minimum of $A_2(k)$ asymmetry2:

$$A_{2,\min} = \min_{k < 50} A_2(k) \quad (12)$$

$$L_{2,\min} = \min_{0 < k < 50} \{k; A_2(k) = A_{2,\min}\} \quad (13)$$

The question is whether they are really related to catchment characteristics. Now, these statistics estimated for 77 discharge data recorded at the gauging stations in Germany are compared with the catchment area as one of the simplest possible indicators of the catchment as shown in Figure 6. $A_{2,\min}$ - area (Figure 6 top) and $L_{2,\min}$ - area (Figure 6 middle) both show a linear relationship with the log-scaled x-axis of catchment area, with positive correlation. There seems also to be a linear relation between $A_{2,\min}$ and $L_{2,\min}$ (Figure 6 bottom) as a consequence of the above relationships.

These results demonstrate that the information extracted from discharge is related to the basic information of its catchment to a certain extent. Since the principal objective is to assess anthropogenic impacts, the idea

Formatted: Font: Italic

Field Code Changed

Field Code Changed

Formatted: Font: Not Italic

introduced now is to use this measure for evaluating the catchment change by calculating chronological changes of $A_{2,\min}$.

3.2 Time Series Analysis with Asymmetry

Temporal change of asymmetry $A_2(k, t)$ is defined $A_2(k, t)$ on the set representing a moving time window of size w .

$$S^*(k, t) = \left\{ (F_Z(z(a))), (F_Z(z(a+k))); t - \frac{w}{2} < a < t + \frac{w}{2} \right\} \quad (14)$$

$$A_2(k, t) = E[-(U_t - 0.5)(U_{t+k} - 0.5)((U_t - 0.5) - (U_{t+k} - 0.5))] \\ = \int_0^1 \int_0^1 -(u_t - 0.5)(u_{t+k} - 0.5)(u_t - u_{t+k})c(u_t, u_{t+k})du_t du_{t+k} \quad (15)$$

where $u_t \in U_t, u_{t+k} \in U_{t+k}, (u_t, u_{t+k}) \in S^*(k, t)$. Then the minimum of $A_2(k)$ and lag k at the minimum of asymmetry at time t are given by

$$A_{2,\min}(t) = \min_{k < 30} A_2(k, t) \quad (16)$$

$$L_{2,\min}(t) = \min_{0 < k < 30} \{k; A_2(k, t) = A_{2,\min}(t)\} \quad (17)$$

Figure 7 shows the temporal changes of $A_{2,\min}(t)$ with window size $w = 3000$ (days) for 7 gauging stations in southwest Germany in addition to the confidence interval calculated for 100 times independently generated Gaussian process.

The comparison of $A_{2,\min}(t)$ from observed discharges with $A_{2,\min}(t)$ from a Gaussian process exhibits (i) the influence of asymmetry in discharge is significantly large as was seen in Figure 5, (ii) The fluctuations of $A_{2,\min}(t)$ of 7 observed discharge time series appear to be bigger than the one calculated for a realization of a Gaussian process and (iii) $A_{2,\min}(t)$ of these 7 discharge records shows a similar trend: there are big drop-downs around 1945 and after 1980 for all the discharges.

245 However, it cannot be ascertained whether this is caused by the simultaneous change of the catchments,
 246 the long term meteorological behavior in the region or just randomness in the stationary process. To
 247 overcome this, temporal behavior of discharge and temperature were first checked by calculating the mean,
 248 the standard deviation and the minimum [of discharge and temperature](#) in a time window centered on time
 249 t defined by

$$\begin{aligned}
 \text{Mean}(t) &= \frac{1}{w} \int_{t-w/2}^{t+w/2} z(a) da & \text{Mean}(t) &= \frac{1}{w} \int_{t-w/2}^{t+w/2} z(a) da \\
 \text{Std}(t) &= \sqrt{\text{Var}(t)} = \frac{1}{w} \left(\int_{t-w/2}^{t+w/2} (z(a) - E[Z(t)])^2 da \right)^{\frac{1}{2}} & \text{Std}(t) &= \sqrt{\text{Var}(t)} = \frac{1}{w} \left(\int_{t-w/2}^{t+w/2} (z(a) - E[Z(t)])^2 da \right)^{\frac{1}{2}} \\
 \text{Min}(t) &= \min \left\{ Z(a); t - \frac{w}{2} < a < t + \frac{w}{2} \right\} & \text{Min}(t) &= \min \left\{ z(a); t - \frac{w}{2} < a < t + \frac{w}{2} \right\}
 \end{aligned}$$

(18)

252 where w is the size of time window. Figure 8 shows the moving average and moving standard deviation of
 253 discharge records with windows size $w = 3000$ [\(days\)](#), but it is hard to say whether the behavior around
 254 1945 and after 1980 is unusual. Figure 9 shows mean and minimum of temperature in the time window of
 255 size 365 [\(days\)](#) which correspond to annual mean and minimum. Roughly speaking, there are certain cold
 256 periods around 1940, 1955 and 1985, which might influence the snow accumulation and melting in the
 257 region, but the relation with [A₂\(k\) asymmetry2](#) is rather obscure.

258 What seems to be a useful outcome from the above exploratory analysis is that (i) the behavior of
 259 [A₂\(k\) asymmetry2](#) is different from catchment to catchment showing a statistical relation with the
 260 catchment area and (ii) temporal behaviors of [A₂\(k\) asymmetry2](#) of 7 discharges time series are dependent
 261 on each other, which implies the existence of a background mechanism common to the region.

262 4. Analysis of hydrological time series with Copula Distance

263 As an alternative to copula asymmetry, which emphasizes the behavior in the corners of copulas, copula
 264 distance is here suggested so that the characteristic behavior can be captured in the entire domain of the

265 copula. Calculating this for each time step for different time series and comparing them hopefully exhibits
 266 the changes of dependence structure and therefore the catchment change.

267 4.1 Introduction of Copula Distance

268 The basic idea behind the copula distance is to apply the Cramér-von Mises type distance

$$269 \quad D = \int_0^1 \int_0^1 (C^*(u_1, u_2) - C(u_1, u_2))^2 du_1 du_2 \quad (19)$$

270 which by design measures the goodness of fit between two distribution functions to two copulas. This type
 271 of distance was tested to measure the difference between empirical and theoretical copulas in the bootstrap
 272 framework for the evaluation of spatial dependence of ground water quality (Bárdossy, 2006). For the
 273 analysis of time series data, it still needs to be carefully thought out how (and which) copulas should be
 274 chosen.

275 4.1.1 Introduction of Copula Distance to single time series

276 In order to apply the concept of copula distance to time series, the adoption of two copulas in different
 277 time scales is considered. An empirical copula can be obtained from an entire time series which contains
 278 the averaged information of all the time points (*global* copula). Another empirical copula can be obtained
 279 for a certain time window of width w centered at time step t (*local* copula). In order to make the concept
 280 clear, two sets containing pairs of ranked values with different time scales are specified.

$$281 \quad S_{\text{global}}(k) = \{(F_Z(z(t))), (F_Z(z(t+k))); t_1 < t < t_n\} \quad S_{\text{global}}(k) = \{(F_Z(z(t))), (F_Z(z(t+k))); t_1 < t < t_n\} \quad (20)$$

$$282 \quad S_{\text{local}}(k, t) = \{(F_Z(z(a))), (F_Z(z(a+k))); t - \frac{w}{2} < a < t + \frac{w}{2}\}$$

$$283 \quad S_{\text{local}}(k, t) = \{(F_Z(z(a))), (F_Z(z(a+k))); t - \frac{w}{2} < a < t + \frac{w}{2}\} \quad (21)$$

284 $S_{\text{local}}(k, t)$ can be interpreted as a moving time window where the reference time t is set to the middle of the
 285 window of size w , while $S_{\text{global}}(k)$ represents a set of the entire time series. Global copula and local copula

Field Code Changed

Formatted: Font: Not Italic

Formatted: Font: Not Italic

Field Code Changed

Field Code Changed

Formatted: Font: Not Italic

Formatted: Font: Not Italic

are the empirical autocopula densities defined on these sets based on Equation (8), there denoted by $c_{global}^*(\mathbf{u})$ and $c_{local}^*(\mathbf{u}, t, w)$ respectively for the n-dimensional case. In this analysis, 3000 days for the time window w and a 3-dimensional copula separated with 1 day gap between each variable are employed. This means that

$$\mathbf{u} = (u_0, u_1, u_2) \quad (22)$$

where $u_0 = F_z(Z(t)), u_1 = F_z(Z(t+1)), u_2 = F_z(Z(t+2))$, then the deviation of local copula from global copula is defined by

$$\Delta c(\mathbf{u}, t) = c_{local}^*(\mathbf{u}, t) - c_{global}^*(\mathbf{u}) \quad \Delta c(\mathbf{u}, t) = c_{local}^*(\mathbf{u}, t) - c_{global}^*(\mathbf{u}) \quad (23)$$

For the first approach, the comparison of dependence structures between entire and local time series is done for detecting unusual dependence structures. To this end, copula distance type1 is defined by taking the copula distance between global and local copulas at each time step t

$$\begin{aligned} D_1(c, t) &= \int_0^1 \dots \int_0^1 (c_{global}^*(\mathbf{u}) - c_{local}^*(\mathbf{u}, t))^2 du_1 \dots du_n \\ &= \int_0^1 \dots \int_0^1 \Delta c(\mathbf{u}, t)^2 du_1 \dots du_n \end{aligned} \quad D_1(c, t) = \int_0^1 \dots \int_0^1 (c_{global}^*(\mathbf{u}) - c_{local}^*(\mathbf{u}, t))^2 du_1 \dots du_n \quad (24)$$

Second, copula distance type-2 is introduced for indicating the point at which the structure of copulas starts to change. For this method, the distance between two local copulas is calculated at two instants:

$$\begin{aligned} D_2(c, t) &= \int_0^1 \dots \int_0^1 \left(c_{local}^*\left(\mathbf{u}, t - \frac{w}{2}\right) - c_{local}^*\left(\mathbf{u}, t + \frac{w}{2}\right) \right)^2 du_1 \dots du_n \\ D_2(c, t) &= \int_0^1 \dots \int_0^1 \left(c_{local}^*\left(\mathbf{u}, t - \frac{w}{2}\right) - c_{local}^*\left(\mathbf{u}, t + \frac{w}{2}\right) \right)^2 du_1 \dots du_n \end{aligned} \quad (25)$$

Note that reference time is set to the middle of both time windows and shifted for $w/2$ days from each other where the size of the time windows is w . Therefore, there is no overlapping part between the two time intervals of these two local copulas. For the comparison, the moving variance is introduced as follows:

$$\begin{aligned}
E[Z(t)] &= \frac{1}{w} \int_{t-w/2}^{t+w/2} z(a) da & E[Z(t)] &= \frac{1}{w} \int_{t-w/2}^{t+w/2} z(a) da \\
Var(t) &= \frac{1}{w} \int_{t-w/2}^{t+w/2} (z(a) - E[Z(t)])^2 da & Var(t) &= \frac{1}{w} \int_{t-w/2}^{t+w/2} (z(a) - E[Z(t)])^2 da
\end{aligned}
\tag{26}$$

Field Code Changed

Figure 10 shows the result of $D_1(t)$, $D_2(t)$ and $Var(t)$ in the moving time window for the normalized discharge time series between 1940 to 2000 at 4 gauging stations located in the main stream of the Rhine (Andernach, Maxau) and its two different tributaries (Cochem, Plochingen) in addition to the 90 % confidence intervals calculated for the Gaussian process fitted to the discharge data of Andernach.

First of all, the values of $D_1(t)$ and $D_2(t)$ at Cochem and Plochingen are bigger and more fluctuating than in general. The reason could be that their catchments and discharges are smaller, thus more sensitive to changes. Second, it can be said that the dependence structure is not homogeneous over the time period, but the local copula clearly deviates from the global copula for certain time periods. For example, the value of $D_1(t)$ is remarkably big around 1947, 1982 and 2000 for all the 4 discharge records (indicated by white arrows). $D_2(t)$ is also big around 1977 for all the data. The signal of $D_2(t)$ implies that a simultaneous change of runoff behavior occurred in this region in 1977, which can be related to the high value of $D_1(t)$ at 1982. ~~$Var(t)$~~ $Var(t)$ is also changing, but a direct relation with $D_1(t)$ and $D_2(t)$ is hard to recognize. Also the confidence interval of the Gaussian process is clearly smaller than the observed one. This indicates the copula distances of the stationary process are small while the nature process is non-stationary and its dependence structure is more varying.

For copula distance type1, the global copula can be considered as an average state of the copula, while the local copula can be regarded as a realization of a possible state of a copula at time step t . This concept can be comparable to variance and leads to a new measure, copula variance, which is the summation of copula distances between global and local copula over the time.

Formatted: Font: Not Italic

$$\cancel{Var_{cop}(c) = \frac{1}{t_n - t_1} \int_{t_1}^{t_n} D_1(c, t) dt} \quad Var_{cop}(c) = \frac{1}{t_n - t_1} \int_{t_1}^{t_n} D_1(c, t) dt
\tag{27}$$

Field Code Changed

Table 1 shows the variance and copula variance calculated for the 4 discharge data. The result demonstrates that copula variance of the time series can be higher, even if the conventional variance is lower for example in case of Maxau.

4.1.2 Copula Distance for two time series

In the previous section, copula variance was defined as a measure of the variability characteristic of the copula itself. Here, it is determined whether covariance can be defined for two copula densities c_1 and c_2 from two time series as copula distance type3, which shows whether the variability characteristic of copulas is related to each other. The measure introduced is:

$$D_3(c_1, c_2, t) = \int_0^1 \dots \int_0^1 \Delta c_1(\mathbf{u}, t) \Delta c_2(\mathbf{u}, t) du_1 \dots du_n \quad (28)$$

where

$$\begin{aligned} \Delta c_1(\mathbf{u}, t) &= c_{1,local}^*(\mathbf{u}, t) - c_{1,global}^*(\mathbf{u}) & \Delta c_1(\mathbf{u}, t) &= c_{1,local}^*(\mathbf{u}, t) - c_{1,global}^*(\mathbf{u}) \\ \Delta c_2(\mathbf{u}, t) &= c_{2,local}^*(\mathbf{u}, t) - c_{2,global}^*(\mathbf{u}) & \Delta c_2(\mathbf{u}, t) &= c_{2,local}^*(\mathbf{u}, t) - c_{2,global}^*(\mathbf{u}) \end{aligned} \quad (29)$$

By its definition, the value of $D_3(t)$ can be related to $D_1(t)$ because $D_3(t)$ compares the deviation of local copulas from global copulas in a similar way to $D_1(t)$ in Equation (26). In order to reduce the influence of $D_1(t)$ on $D_3(t)$, copula distance type4 is introduced as a normalized measure bounded between -1 and 1 analogous to correlation.

$$D_4(c_1, c_2, t) = \frac{D_3(c_1, c_2, t)}{\sqrt{D_1(c_1, t)} \cdot \sqrt{D_1(c_2, t)}} \quad (30)$$

where $|D_4(c_1, c_2, t)| \leq 1$. For comparison, covariance and correlation in a moving window are introduced for two random variables $Z_1(t)$ and $Z_2(t)$ as follows:

$$\text{Cov}(t) = \int_{t-w/2}^{t+w/2} (z_1(a) - E[Z_1(t)])(z_2(a) - E[Z_2(t)]) da \quad \text{Cov}(t) = \int_{t-w/2}^{t+w/2} (z_1(a) - E[Z_1(t)])(z_2(a) - E[Z_2(t)]) da \quad (31)$$

$$Corr(t) = \frac{Cov(t)}{\sqrt{Var(Z_1(t))} \cdot \sqrt{Var(Z_2(t))}} \quad (32)$$

Field Code Changed

Figure 11 shows the copula distance between two time series $D_3(t)$ and $D_4(t)$ in addition to the covariance and correlation in a moving time window.

First, it can be said that the behavior of covariance and correlation in a moving window are different from $D_3(t)$ and $D_4(t)$. This implies these two copula based statistics exhibit different properties of the time series from ordinary statistics. Second, $D_3(t)$ shows high values around 1947, 1982 and 2000, which is similar to the case of $D_1(t)$ in Fig. 10. This indicates that unusual states of copulas in 4 discharge time series can be related to each other. Third, $D_4(t)$ is in general high except for the period around 1970 and 1990. This means, the temporal behavior of dependence structures for these 4 discharges are actually similar except for these periods even if $D_1(t)$ and $D_3(t)$ are small.

Copula covariance and copula correlation can be defined similar to copula variance in order to quantify the overall behavior of two time series.

$$Cov_{cop}(c_1, c_2) = \frac{1}{t_2 - t_1} \int_{t_1}^{t_2} D_3(t) dt \quad Cov_{cop}(c_1, c_2) = \frac{1}{t_2 - t_1} \int_{t_1}^{t_2} D_3(t) dt \quad (33)$$

Field Code Changed

$$Corr_{cop}(c_1, c_2) = \frac{Cov_{cop}(c_1, c_2)}{\sqrt{Var_{cop}(c_1)} \cdot \sqrt{Var_{cop}(c_2)}} \quad Corr_{cop}(c_1, c_2) = \frac{Cov_{cop}(c_1, c_2)}{\sqrt{Var_{cop}(c_1)} \cdot \sqrt{Var_{cop}(c_2)}} \quad (34)$$

Field Code Changed

where $|Corr_{cop}(c_1, c_2)| \leq 1$ and its derivation can be found in appendix A. In Table 2, these copula based statistics are compared with ordinary statistics. For example, Cochem and Plochingen are located remotely in different tributaries, thus covariance and correlation are lower than the others, but copula covariance and copula correlation are not the lowest.

The measures using copula distance are different from the conventional statistics. This behavior can be explained by the fact that the autocopula has more substantial information about temporal dependence

Formatted: Font: Not Bold

Formatted: Font: Not Bold

structure than the autocorrelation. Using these measures might enable us to take advantage of a different way of seeing the dependence between time series.

What is new in the analysis of this section is that (i) measures based on copula distance show the different properties of time series in comparison to conventional statistics and (ii) there are significant signals of copula distances for certain time periods in common to all the discharge data.

4.2 Copula based Stochastic Analysis with API and a Hydrological Model

The difficulty of analyzing discharge time series in order to detect catchment change is that it is not clear whether the temporal change of stochastic information is caused by catchment change or merely by random behavior of precipitation. To gain an understanding of this process, we attempted to eliminate the influence of precipitation using, first, an Antecedent Precipitation Index (API) for comparison with discharge, second, using a hydrological model with the parameter sets calibrated and fixed for the entire simulation time period.

4.2.1 Copula Distance Analysis with API

An API time series, which is generated from observed precipitation time series and behaves similarly to discharge, is used instead of precipitation.

$$\cancel{API(t+1)} = \cancel{\alpha API(t) + P(t+1)} \quad \underline{API(t+1) = \alpha API(t) + P(t+1)} \quad (35)$$

where $P(t)$ is daily precipitation $\cancel{[(\text{mm/day})]}$, $\underline{API(t)}$ is time series of API $\cancel{[(\text{mm/day})]}$ and $\alpha = 0.85$ was chosen. The assumption for this method is that the API time series has the stochastic information purely originated from the precipitation, while observed discharge is influenced by both catchment and precipitation characteristics. If the stochastic information derived from these two data sets is the same, this indicates that the stochastic turbulence is originating from precipitation; otherwise the change is from the catchment.

Field Code Changed

For this investigation, precipitation data was carefully chosen for 4 regions (northwest, northeast, southwest and central) of Baden-Württemberg (Germany) so that they have several almost continuous daily records between 1935 and 2005. Figure 12 shows the locations of measuring stations. The precipitation time series were aggregated into one for each region by taking their daily average, then 4 API time series were calculated in total by Eq. ~~uation(35)(35)(35)~~. Figure 13 shows the resulting copula distances $D_1(t), D_2(t)$ and moving average ~~$\text{Var}(t)$~~ $\text{Var}(t)$ for API time series with the 90% confidence intervals of the Gaussian process. Figure 14 shows the result of copula distances $D_3(t), D_4(t)$ and moving covariance and correlation for API time series.

What can be recognized first from Fig. ~~ure~~ 13 is that the magnitudes of $D_1(t)$ and $D_2(t)$ are smaller than the case of discharge. This is considered to be a result of aggregation of precipitation time series and adoption of API, but some signals can be still identified: $D_1(t)$ around 1947 and 2000 is high, but not as high for 1982. The signal of $D_2(t)$ which was detected around 1977 in Fig. ~~ure~~ 11 does not seem to exist for API. This is even more clear for $D_3(t)$ in Fig. ~~ure~~ 14 in that there is no common change of the dependence structure around 1982 in API time series. This is interesting due to the following implications:

(i) the noises of $D_1(t)$ in ~~Fig. 13~~ ~~Fig. 13~~ were reduced and signals in common were amplified (ii) the unusual state of the copula around 1982 is not caused by precipitation, but could be caused by the catchment change.

For further verification, copula distance type3 and type4 between discharge and API time series were calculated as shown in Fig. ~~ure~~ 15. This result also shows there is no clear relation between API and discharge time series around 1982.

4.2.2 Copula based analysis with a hydrological model

In this section, simulated discharges time series are generated by a conceptual hydrological model, HBV (Bergström 1976 ; Bergström, Singh, and others 1995)-, which takes daily precipitation and temperature

Field Code Changed

Formatted: Font: Not Bold

Formatted: Font: Not Bold

412 records as input and simulates discharges for smaller catchments as an example of discharge, to compare
413 with observed discharge, in order to check if differences might occur due to the method.

414 Thus the idea behind this methodology is similar to the case of API: a hydrological model with the
415 parameters fixed for the entire time period represents the catchment not influenced by anthropogenic
416 impacts. Then, the discharges simulated by this model should not depend on catchment change, while
417 observed discharge is assumed to be influenced by both catchment and precipitation.

418 For the study area, the Upper Neckar Catchment was chosen as shown in Fig. 12. One parameter set
419 needed for this model constitutes of 13 parameters which are calibrated based on the Nash–Sutcliffe model
420 efficiency coefficient using the simulated annealing algorithm for the period between 1960 and 2000. Then,
421 30 parameter sets are independently calibrated in total and, subsequently, 30 simulated discharges time
422 series are generated to compare with one observed discharge.

423 Figure 16 shows the result of copula based analysis calculated for single time series
424 $(D_1(t), D_2(t), A_{2,\min}(t))$. It can be seen that $A_{2,\min}(t)$ in Fig. 16 (top) that (i) fluctuations of $A_{2,\min}(t)$
425 of observed and simulated discharge are locally identical. This implies that the short term behavior of
426 $A_{2,\min}(t)$ is originated from the temporal behavior of precipitation but (ii) there exists a change of trend
427 around 1976: $A_{2,\min}(t)$ of observed discharge is slightly bigger than simulated before 1976, while
428 $A_{2,\min}(t)$ of observed discharge clearly undershoot the simulated ones of after 1976. This change of trend
429 was also seen in the previous analyses ($D_2(t)$ in Fig. 10). Furthermore, $D_1(t)$ in Fig. 16 (middle) is
430 high before 1976 which indicates the state of the copula is different from the rest, while the result of
431 simulated discharges does not show such tendency. $D_2(t)$ in Fig. 16 (bottom) indicates the change of
432 dependence structure happened around 1970 and 1977. These results using the HBV model indicate the
433 change of the dependence structure detected using copulas around 1976 is not caused by the random
434 behavior of precipitation, but by the behavior of the catchment itself.

435 The fact and the notion obtained in this section is that (i) both results from API and HBV based on
436 copula measures indicate that the catchment changed around 1976 and (ii), by comparing the simulated
437 discharge with observed discharge, the origin of the change of stochastic~~ly~~ information can be assessed.
438

439 Conclusion

440 In this paper the application of copulas for hydrological time series data is newly explored for the
441 detection of catchment characteristics and their temporal changes.

442 1. A Copula based measure of asymmetry, ~~asymmetry~~ $A_1(k)$ and $A_2(k)$, was defined and newly applied
443 for the identification of catchment characteristics. Indeed, it was presumed that asymmetry2 is related to
444 the runoff characteristics.

445 2. The relation between ~~the minimum of~~ asymmetry2 and catchment characteristics was tested for 77
446 discharge records. $A_{2,min}$ Asymmetry2 has a certain relation especially with the size of catchments and this
447 strengthens the notion that asymmetry2 of discharge data can be used to describe ~~as a statistic to explain~~
448 the catchment characteristic and state.

449 3. ~~Temporal change of asymmetry2~~ $A_{2,min}(t)$ was defined for evaluating the temporal change of
450 asymmetry2 and calculated as an indicator ~~index~~ of the catchment state. The result ~~and~~ indicates
451 $A_{2,min}(t)$ ~~demonstrated it~~ keeps changing coincidentally with time. However, it is difficult to explain the
452 causality, at least, by long term behavior of discharge and temperature time series.

453 4. A method based on copula distance was examined for the investigation of temporal behavior of
454 hydrological time series. This measure can detect the time period where dependence structure is unusual
455 and its interdependency between different time series. Clear signals were detected that the dependence
456 structure is unusual for a certain time period and this ~~is~~ signal was not found by investigating the time series
457 with variance, covariance or correlation.

458 | 5. API time series were ~~calculated~~^{generated} for each region in the Baden-Württemberg state and
459 simulated discharge time series were generated using the HBV model for the Upper Neckar Catchment.
460 These are the data not influenced by catchment change, thus compared with observed discharge to assess
461 the anthropogenic impacts. The results showed that there was a signal detected only in the observed
462 discharge around 1982, but not in the API or simulated time series, which implies the anthropogenic
463 impacts on the catchment. Also it was shown in the results of copula asymmetry that the trend clearly
464 changed around 1976.

465 The results of copula based analysis of hydrological time series seem to support the assumption that the
466 catchment had started to change around 1976 and stayed unusual until 1990. These changes could
467 correspond to the construction of flood retention basins started around 1982 (Lammersen et al., 2002) and
468 ecological flooding strategy, which let small floods to happen for the rehabilitation of ecological systems
469 in the floodplain, introduced in the Upper Rhine since 1989 (Siepe, 2006).

470 Copulas can be seen as an alternative method to analyze hydrological time series data by focusing on the
471 dependence structure, but further exploratory applications and theoretical developments are expected. The
472 copula based measures introduced in this study can be related to the potential model uncertainty, that is,
473 how much the natural system is varying. Empirical autocopula analysis is a more data driven approach
474 which retains more information than the copulas estimated with parametric methods, but it is also
475 numerically demanding. The effective way to analyze time series and build up a time series model based
476 on copulas can be further explored.

477

Field Code Changed

Field Code Changed

Field Code Changed

478 **Appendix A**

479 Suppose that a random variable at time t is denoted as $X(t)$ and $c_X(\mathbf{u}, t)$ is an autocopula obtained from
 480 $X(t)$. Assuming $c_{X,\text{mean}}(\mathbf{u})$ as an average state of $c_X(\mathbf{u}, t)$, deviation of copula $\Delta c_X(\mathbf{u}, t)$ at
 481 time t is defined by

$$482 \quad \Delta c_X(\mathbf{u}, t) = c_X(\mathbf{u}, t) - c_{X,\text{mean}}(\mathbf{u}) \quad (\text{A1})$$

483 For the empirical case, $c_X(\mathbf{u}, t)$ and $c_{X,\text{mean}}(\mathbf{u})$ can be regarded as local copula and global copula
 484 respectively similar to Equation (29)(29)(29). Since global and local copula are empirical copula density
 485 as defined in Equation (8)(8)(8), $\Delta c_X(\mathbf{u}, t)$ can be regarded as a vector of values on finite number of
 486 grids:

$$487 \quad \Delta \mathbf{c}_X(t) = (\Delta c_{X,1}(t), \Delta c_{X,2}(t), \dots, \Delta c_{X,i}(t), \dots, \Delta c_{X,N}(t)) \quad (\text{A2})$$

488 where $\Delta c_{X,i}(t)$ denotes the value of copula density at i -th grid and N is the number of grids. From
 489 Cauchy-Schwarz inequality

$$490 \quad \|\Delta \mathbf{c}_X(t)\| \|\Delta \mathbf{c}_Y(t)\| \geq \left| \langle \Delta \mathbf{c}_X(t), \Delta \mathbf{c}_Y(t) \rangle \right|^2 \quad (\text{A3})$$

491 where $\|\Delta \mathbf{c}_X(t)\|$ is norm and $\langle \Delta \mathbf{c}_X(t), \Delta \mathbf{c}_Y(t) \rangle$ is inner product of vector $\Delta \mathbf{c}_X(t)$ and $\Delta \mathbf{c}_Y(t)$. Then

$$492 \quad \begin{aligned} \|\Delta \mathbf{c}_X(t)\| &= \sum_{i=1}^N \Delta c_{X,i}(t)^2 \\ &= \int_0^1 \dots \int_0^1 (\Delta c_X(\mathbf{u}, t))^2 du_1 \dots du_n = D_1(c_X, t) \end{aligned} \quad (\text{A4})$$

$$493 \quad \begin{aligned} &\left| \langle \Delta \mathbf{c}_X(t), \Delta \mathbf{c}_Y(t) \rangle \right|^2 \\ &= \langle \Delta \mathbf{c}_X(t), \Delta \mathbf{c}_Y(t) \rangle = \sum_{i=1}^N \Delta c_{X,i}(t) \cdot \Delta c_{Y,i}(t) \\ &= \int_0^1 \dots \int_0^1 \Delta c_X(\mathbf{u}, t) \Delta c_Y(\mathbf{u}, t) du_1 \dots du_n = D_3(c_X, c_Y, t) \end{aligned} \quad (\text{A5})$$

$$\frac{\left\langle \Delta \mathbf{c}_X(t), \Delta \mathbf{c}_Y(t) \right\rangle^2}{\left\| \Delta \mathbf{c}_X(t) \right\| \left\| \Delta \mathbf{c}_Y(t) \right\|} = \frac{D_3(c_X, c_Y, t)^2}{D_1(c_X, t) \cdot D_1(c_Y, t)} = D_4(c_X, c_Y, t)^2 \leq 1 \quad (\text{A6})$$

Field Code Changed

Therefore $\left| D_4(c_X, c_Y, t) \right| \leq 1$ in Eq. (30). Above inequality is valid for certain time point t and summing up Eq. (A6) for all the time steps t leads to

$$\sum_{t=1}^T \left(\left\| \Delta \mathbf{c}_X(t) \right\| \cdot \left\| \Delta \mathbf{c}_Y(t) \right\| \right) \geq \sum_{t=1}^T \left| \left\langle \Delta \mathbf{c}_X(t), \Delta \mathbf{c}_Y(t) \right\rangle \right|^2 \quad (\text{A7})$$

Field Code Changed

where T is the number of time steps. $\left\| \Delta \mathbf{c}_X(t) \right\|$ is a norm and can be denoted for simplicity as

$x_t = \left\| \Delta \mathbf{c}_X(t) \right\|$. Then

$$\sum_{t=1}^T \left(\left\| \Delta \mathbf{c}_X(t) \right\| \cdot \left\| \Delta \mathbf{c}_Y(t) \right\| \right) = \langle \mathbf{x}, \mathbf{y} \rangle \quad (\text{A8})$$

Field Code Changed

where $\mathbf{x} = (x_1, x_2, \dots, x_T)$, $\mathbf{y} = (y_1, y_2, \dots, y_T)$ for $t = 1 \dots T$. Again from Cauchy-Schwarz inequality

$$\left| \langle \mathbf{x}, \mathbf{y} \rangle \right|^2 \leq \left\| \mathbf{x} \right\| \cdot \left\| \mathbf{y} \right\| \quad (\text{A9})$$

Field Code Changed

$$\begin{aligned} \left\| \mathbf{x} \right\| \cdot \left\| \mathbf{y} \right\| &= \sum_{t=1}^T x_t^2 \cdot \sum_{t=1}^T y_t^2 = \sum_{t=1}^T \left\| \Delta \mathbf{c}_X(t) \right\|^2 \cdot \sum_{t=1}^T \left\| \Delta \mathbf{c}_Y(t) \right\|^2 \\ &= \sum_{t=1}^T D_1(c_X, t)^2 \cdot \sum_{t=1}^T D_1(c_Y, t)^2 = T^2 \cdot \text{Var}_{\text{cop}}(c_X) \cdot \text{Var}_{\text{cop}}(c_Y) \end{aligned}$$

Formatted: Text

$$\begin{aligned} \left\| \mathbf{x} \right\| \cdot \left\| \mathbf{y} \right\| &= \sum_{t=1}^T x_t^2 \cdot \sum_{t=1}^T y_t^2 = \sum_{t=1}^T \left\| \Delta \mathbf{c}_X(t) \right\|^2 \cdot \sum_{t=1}^T \left\| \Delta \mathbf{c}_Y(t) \right\|^2 \\ &= \sum_{t=1}^T D_1(c_X, t)^2 \cdot \sum_{t=1}^T D_1(c_Y, t)^2 = T^2 \cdot \text{Var}_{\text{cop}}(c_X) \cdot \text{Var}_{\text{cop}}(c_Y) \end{aligned} \quad (\text{A10})$$

Field Code Changed

$$\begin{aligned} \langle \mathbf{x}, \mathbf{y} \rangle &= \sum_{t=1}^T (x_t \cdot y_t) = \sum_{t=1}^T \left(\left\| \Delta \mathbf{c}_X(t) \right\| \cdot \left\| \Delta \mathbf{c}_Y(t) \right\| \right) \geq \sum_{t=1}^T \left| \left\langle \Delta \mathbf{c}_X(t), \Delta \mathbf{c}_Y(t) \right\rangle \right|^2 \\ &= \sum_{t=1}^T D_{3,XY} = T \cdot \text{Cov}_{\text{cop}}(c_X, c_Y) \end{aligned}$$

$$\begin{aligned} \langle \mathbf{x}, \mathbf{y} \rangle &= \sum_{t=1}^T (x_t \cdot y_t) = \sum_{t=1}^T \left(\left\| \Delta \mathbf{c}_X(t) \right\| \cdot \left\| \Delta \mathbf{c}_Y(t) \right\| \right) \geq \sum_{t=1}^T \left| \left\langle \Delta \mathbf{c}_X(t), \Delta \mathbf{c}_Y(t) \right\rangle \right|^2 \\ &= \sum_{t=1}^T D_3(c_X, c_Y, t) = T \cdot \text{Cov}_{\text{cop}}(c_X, c_Y) \end{aligned} \quad (\text{A11})$$

Field Code Changed

507 Then $\left|\left\langle \mathbf{x}, \mathbf{y} \right\rangle\right|^2 \leq \left\|\mathbf{x}\right\|\left\|\mathbf{y}\right\|$ indicates

508

$$\begin{aligned} \left|Cov_{cop}\left(c_X,c_Y\right)\right|^2 &\leq Var_{cop}\left(c_X\right)Var_{cop}\left(c_Y\right) \\ \left|Corr_{cop}\right| &= \frac{Cov_{cop}\left(c_X,c_Y\right)}{\sqrt{Var_{cop}\left(c_X\right)}\cdot\sqrt{Var_{cop}\left(c_Y\right)}} \leq 1 \end{aligned}$$

509

$$\begin{aligned} \left|Cov_{cop}\left(c_X,c_Y\right)\right|^2 &\leq Var_{cop}\left(c_X\right)Var_{cop}\left(c_Y\right) \\ \left|Corr_{cop}\right| &= \frac{Cov_{cop}\left(c_X,c_Y\right)}{\sqrt{Var_{cop}\left(c_X\right)}\cdot\sqrt{Var_{cop}\left(c_Y\right)}} \leq 1 \end{aligned} \tag{A12}$$

510

511

Field Code Changed

512 **Acknowledgment**

513 | Fundamental research of this paper was initiated by the [BfG](#) (German Federal Institute of Hydrology)
514 with financial support. Special thanks are given to the Global Runoff Data Centre (GRDC) in Germany for
515 offering the discharge data and the German Meteorological Service (DWD) for precipitation and
516 temperature data. The authors thank the reviewers for their care in examining this work.

517 **References**

518 Bárdossy, a., Pegram, G., 2009. Copula based multisite model for daily precipitation simulation. Hydrol.
519 Earth Syst. Sci. Discuss. 6, 4485–4534. doi:10.5194/hessd-6-4485-2009

520 Bárdossy, A., 2006. Copula-based geostatistical models for groundwater quality parameters. Water Resour.
521 Res. 42, W11416. doi:10.1029/2005WR004754

522 Bárdossy, A., Li, J., 2008. Geostatistical interpolation using copulas. Water Resour. Res. 44, W07412.
523 doi:10.1029/2007WR006115

524 Bergström, S., 1976. Development and application of a conceptual runoff model for Scandinavian
525 catchments, Bulletin Series A, A]: [Bulletin series. Department of Water Resources Engineering, Lund
526 Institute of Technology, University of Lund.

527 Bergstrom, S., 1995. The HBV Model. Singh, V.P. (Ed.), Comput. Model. Watershed Hydrol. 443–476.

528 Box, G.E.P., Jenkins, G.M., 1976. Time series analysis: forecasting and control, revised ed. Holden-Day,
529 San Francisco, USA.

530 Brahimi, B., Chebana, F., Necir, A., 2014. Copula representation of bivariate L-moments: a new
531 estimation method for multiparameter two-dimensional copula models. Statistics (Ber). 1–25.

532 De Michele, C., Salvadori, G., 2003. A Generalized Pareto intensity-duration model of storm rainfall
533 exploiting 2-Copulas. J. Geophys. Res. Atmos. 108, 4067. doi:10.1029/2002JD002534

534 Gao, P., Geissen, V., Ritsema, C., Mu, X.-M., Wang, F., 2012. Impact of climate change and
535 anthropogenic activities on stream flow and sediment discharge in the Wei River basin, China. Hydrol.
536 Earth Syst. Sci. Discuss. 9, 3933–3959. doi:10.5194/hessd-9-3933-2012

537 Grimaldi, S., 2004. Linear parametric models applied to daily hydrological series. J. Hydrol. Eng. 9, 383–
538 391. doi:10.1061/(ASCE)1084-0699(2004)9:5(383)

539 Huang, N.E., Shen, Z., Long, S.R., Wu, M.C., Shih, H.H., Zheng, Q., Yen, N.-C., Tung, C.C., Liu, H.H.,
540 1998. The empirical mode decomposition and the Hilbert spectrum for nonlinear and non-stationary time
541 series analysis. Proc. R. Soc. London. Ser. A Math. Phys. Eng. Sci. 454, 903–995.

542 Joe, H., 1997. Multivariate models and multivariate dependence concepts. Chapman&Hall, London.

543 Karlsson, I.B., Sonnenborg, T.O., Jensen, K.H., Refsgaard, J.C., 2014. Historical trends in precipitation
544 and stream discharge at the Skjern River catchment, Denmark. *Hydrol. Earth Syst. Sci.* 18, 595–610.
545 doi:10.5194/hess-18-595-2014

546 Lammersen, R., Engel, H., Van de Langemheen, W., Buiteveld, H., 2002. Impact of river training and
547 retention measures on flood peaks along the Rhine. *J. Hydrol.* 267, 115–124. doi:10.1016/S0022-
548 1694(02)00144-0

549 Li, J., 2010. Application of copulas as a new geostatistical tool. PhD Thesis. Nr. 187. University of
550 Stuttgart, Germany

551 Nelsen, R.B., 2006. An Introduction to Copulas. Springer, New York. doi:10.1007/0-387-28678-0

552 Pettitt, A.N., 1979. A non-parametric approach to the change-point problem. *Appl. Stat.* 126–135.

553 Samaniego, L., Bárdossy, A., Kumar, R., 2010. Streamflow prediction in ungauged catchments using
554 copula-based dissimilarity measures. *Water Resour. Res.* 46, W02506. doi:10.1029/2008WR007695

555 Serfling, R., Xiao, P., 2007. A contribution to multivariate L-moments: L-comoment matrices. *J. Multivar.*
556 *Anal.* 98, 1765–1781. doi:10.1016/j.jmva.2007.01.008

557 Sharifdoost, M., Mahmoodi, S., Pasha, E., 2009. A statistical test for time reversibility of stationary finite
558 state Markov chains. *Appl. Math. Sci.* 52, 2563–2574.

559 Siepe, A., 2006. Dynamische Überflutungen am Oberrhein : Entwicklungs-Motor für die Auwald-Fauna.
560 Stand 149–158.

561 Singh, S.K., McMillan, H., Bárdossy, A., 2013. Use of the data depth function to differentiate between
562 case of interpolation and extrapolation in hydrological model prediction. *J. Hydrol.* 477, 213–228.
563 doi:10.1016/j.jhydrol.2012.11.034

564 Sklar, A., 1959. Fonctions de répartition à n dimensions et leurs marges, Publications de l’Institut de
565 statistique de l’Université de Paris. Publications de l’Institut de Statistique de L’Université de Paris 8.

566 Sugimoto, T., 2014. Copula based stochastic analysis of discharge time series. PhD Thesis. Nr. 232.
567 University of Stuttgart, Germany

568 Wu, C.S., Yang, S.L., Lei, Y.P., 2012. Quantifying the anthropogenic and climatic impacts on water
569 discharge and sediment load in the Pearl River (Zhujiang), China (1954-2009). *J. Hydrol.* 452-453, 190–
570 204. doi:10.1016/j.jhydrol.2012.05.064

571

572

573 **Table 111.** Variance and copula variance calculated for 4 discharge time series

574 (ANDE:Andernach, COCH:Cochem, MAXA:Maxau, PLOC:Plochingen)

575
576

	ANDE	COCH	MAXA	PLOC
Var	1.79	2.24	1.75	2.72
Var _{cop} $\times 10^{-5}$	3.01	1.64	5.39	1.27

577

578 **Table 222.** Covariance, correlation, copula covariance and copula correlation between 4 discharge data

579 (AN:Andernach, CO:Cochem, MA:Maxau, PL:Plochingen)

580
581

	AN-CO	AN-MA	AN-PL	CO-MA	CO-PL	MA-PL
Cov	1.68	1.60	1.33	1.38	1.31	1.41
Cor	0.84	0.90	0.60	0.70	0.53	0.64
Cov _{cop} $\times 10^{-5}$	4.90	3.40	3.39	7.16	9.90	5.47
Cor _{cop}	0.60	0.77	0.46	0.71	0.60	0.59

582

583 **Table 333.** Variance and copula variance calculated for API time series of 4 regions in the Baden-

584 Württemberg state of Germany (C: Central, SW: South-West, NW: North-West, NE: North-East)

585

586
587

	C	SW	NW	NE
Var	1.70	1.66	1.72	1.78
Var _{cop} $\times 10^{-5}$	3.00	4.02	3.35	3.21

588

589
590 **Table 444.** Covariance, correlation, copula covariance and copula correlation between API time series

591 from 4 regions in the Baden-Württemberg state of Germany

592
593

	C-SW	C-NW	C-NE	SW-NW	SW-NE	NW-NE
Cov	1.35	1.33	1.44	1.25	1.41	1.42
Cor	0.80	0.77	0.84	0.74	0.84	0.83
Cov _{cop} $\times 10^{-5}$	1.46	1.16	8.94	4.42	1.11	8.80
Cor _{cop}	0.36	0.29	0.29	0.09	0.26	0.24

594

Formatted: Font: Bold

Formatted: Font: Bold

Formatted: Font: Bold

Formatted: Left

Formatted: Font: Not Italic

Formatted: Font: Not Italic

Formatted: Font: Bold

Formatted: Font: Not Italic

Formatted: Font: Not Italic

Formatted: Font: Not Italic

Formatted: Font: Not Italic

Formatted: Font: Not Italic

Formatted: Font: Bold

Formatted: Font: Not Italic

Formatted: Font: Not Italic

Formatted: Font: Not Italic

Formatted: Font: Not Italic

Formatted: Font: Not Italic

Formatted: Font: Not Italic

Formatted: Font: Not Italic

Formatted: Font: Not Italic

595 Figure Captions

596

597 **Fig. 1.** Locations of 7 discharge gauging stations in the Upper Rhine Region

598 **Fig. 2.** Visualization of $a_1(u_t, u_{t+k}) = (u_t - 0.5)(u_{t+k} - 0.5)((u_t - 0.5) + (u_{t+k} - 0.5))$ (left) and
599 $a_2(u_t, u_{t+k}) = (u_t - 0.5)(u_{t+k} - 0.5)((u_t - 0.5) - (u_{t+k} - 0.5))$ (right) which displays the contribution of single
600 realization of (U_t, U_{t+k}) to asymmetry functions

601 $A_1(k) = E[(U_t - 0.5)(U_{t+k} - 0.5)((U_t - 0.5) + (U_{t+k} - 0.5))]$ and

602 $A_2(k) = E[-(U_t - 0.5)(U_{t+k} - 0.5)((U_t - 0.5) - (U_{t+k} - 0.5))]$

603 **Fig. 3.** Sketch of the transformation of the values from sample hydrograph (left) to the points on scatterplot
604 of ranks (right): empirical copula calculated from two values separated by time lag $k = 1$ (days) in a
605 discharge time series of Andernach where rank correlation is 0.9870, $A_1(k = 1) = -0.0002398$ and
606 $A_2(k = 1) = -0.00011037$. The possible combinations of high and low values, which has large impacts on
607 asymmetry, are numbered: (1) low to high, (2) high to high, (3) high to low, (4) low to low. Negative
608 contribution to A_2 is drawn with red circle and positive contribution with blue oval.

609 **Fig. 4.** Annual cycles of mean discharge measured at seven sites in the Rhine basin after smoothing (left)
610 and annual cycle of standard deviation after smoothing (right)

611 **Fig. 5.** Discharge time series measured at seven sites in the Rhine basin between 1950 and 1955 before
612 applying normalization (upper left) and after applying normalization (upper right). $A_2(k)$ calculated for
613 entire time series before applying normalization (bottom left) and after applying normalization (bottom
614 right) with 90% confidence intervals (grey) calculated for 100 realizations of Gaussian process (dashed
615 line is $A_2(k)$ calculated for one of the realization of Gaussian process).

616 **Fig. 6.** Relation between asymmetry of discharge data and catchment characteristics: $A_{2,min}$ of discharge
617 and catchment area (top), $A_{2,min}$ of discharge and catchment area (middle), $A_{2,min}$ of discharge and $L_{2,min}$ of
618 discharge (bottom)

619 **Fig. 7.** Temporal change of asymmetry2 : $A_{2,min}(t)$ for 7 discharge records and, for comparison, confidence
620 intervals calculated from the Gaussian process (90% confidence interval with grey color and 60%
621 confidence interval with dark grey color) and one of its realizations (dashed line)

622 **Fig. 8.** Moving average and standard deviation of the 7 daily discharge records for the window size $w =$
623 3000 (days)

624 **Fig. 9.** Annual minimum (upper panel) and mean of aggregated daily temperature (lower pannel) in the
625 Baden-Württemberg state of Germany

Formatted: Do not check spelling or grammar, Lowered by 5 pt

Fig. 10. Copula distances of discharge time series in moving time window: variance (top), distance type1 (middle) and distance type2 (bottom), each panel containing the 80% confidence interval of Gaussian process and one of its realization (dashed line). The arrows point 1947, 1982, 2000 and 1977 in which the clear signals of anomalies are detected for all four discharge time series: Andernach(ANDE), Cochem(COCH), Maxau(MAXA) and Plochingen(PLOC)).

Fig. 11. Copula distances of discharge time series in moving time window: covariance (top), correlation (second), copula distance type3 (third) and copula distance type4 (bottom). The arrows point 1947, 1982 and 2000 in which the clear signals of anomalies are detected for the comparisons between 4 discharge time series: Andernach(ANDE), Cochem(COCH), Maxau(MAXA), Plochingen(PLOC)

Fig. 12. Locations of the precipitation gauge stations within Baden-Württemberg (Germany) indicated by coloured circles. Upper Neckar catchment is identified by the light green area and the location of the gauging station is indicated by a square

Fig. 13. Copula distances of API time series in moving time window: variance (top), copula distance type1 (middle) and copula distance type2 (bottom) where 'C' denotes central, 'SW' denotes southwest, 'NW' denotes northwest and 'NE' denotes northeast part of the Baden-Württemberg State of Germany, each containing 80% confidence interval of Gaussian process and one of its realization (dashed line). The arrows indicate the years in which anomalies are detected in the previous analysis (Fig. 10)

Fig. 14. Copula distances of API time series in moving time window: covariance (top), correlation (second), copula distance type3 (third) and copula distance type4 (bottom). The arrows indicate the years in which anomalies are detected in the previous analysis (Fig. 11)

Fig. 15. Copula distance type3 (top) and type4 (bottom) between 4 discharge and 1 API time series which is aggregated for all the daily precipitations depicted in Fig. 12. The arrows indicate the years in which anomalies are detected in the previous analysis (Fig. 11)

Fig. 16. Copula asymmetry and copula distances for 30 simulated and one observed discharge time series at Plochingen between 1965 and 2000: $A_{2,min}$ for the time lag $k = 2$ days (top), copula distance type1 (middle), copula distance type2 (bottom)

Figure 1 Locations of 7 discharge gauging stations in the Upper Rhine Region

Figure 2 Visualization of the functions which displays the contribution of a realization of (U_t, U_{t+k}) to *asymmetry1* (left) and *asymmetry2* (right)

Figure 3 Sketch of the transformation from sample hydrograph (left) to empirical copula (right): Scatterplot of ranks are calculated from two values separated by time lag $k = 1$ [days] in a discharge time series of Andernach where *rank correlation* = 0.9870, $A_1(k = 1) = 0.0002398$ and $A_2(k = 1) = 0.00011037$. The possible combinations of high and low values, which has large impacts on asymmetry, are numbered (1) low to high, (2) high to high (3) high to low (4) low to low. Negative contribution to *asymmetry2* is drawn with red circle, positive contribution with blue circle.

Figure 4 Annual cycle of mean discharge after smoothing (left) and annual cycle of standard deviation after smoothing (right)

Figure 5 Discharge time series between 1950 and 1955 before applying normalization (upper left) and after applying normalization (upper right). The variation of asymmetry2 function calculated for entire time series before applying normalization (bottom left) and after applying normalization (bottom right) with 90% confidence intervals (grey) calculated for 100 realizations of Gaussian process (dashed line is $A_2(k)$ calculated for one of the realization of Gaussian process).

Figure 6 Relation between Asymmetry and catchment characteristics: minimum of asymmetry2 of discharge and catchment area (top), lag at minimum of asymmetry2 of discharge and catchment area (middle), minimum of asymmetry2 of discharge and lag at minimum of asymmetry2 of discharge (bottom)

Figure 7 Temporal change of minimum of asymmetry2 for 7 discharge records and confidence intervals calculated from the Gaussian process (90% confidence interval with grey color and 60% confidence interval with dark grey color) and one of its realizations (dashed line)

Figure 8 Moving average and standard deviation of the 7 daily discharge records for the window size $w=3000$

Figure 9 Annual minimum and mean of aggregated daily temperature in the Baden-Württemberg state of Germany

Figure 10 Copula distances of discharge time series in moving time window: moving variance (top), distance type1 (middle) and distance type2 (bottom) with 80% confidence interval of Gaussian process and one of its realization (dashed line)

Figure 11 Copula distances of discharge time series in moving time window: moving covariance (top), moving correlation (second), distance type3 (third) and distance type4 (bottom)

Figure 12 Locations of the precipitation gauge stations within the Baden-Württemberg (Germany) indicated by coloured circles. Upper Neckar catchment is drawn with green area and the location of gauging station is drawn with a square

Figure 13 Copula distances of API time series in moving time window: moving variance (top), copula distance type1 (middle) and copula distance type2 (bottom) where 'C' denotes central, 'SW' denotes southwest, 'NW' denotes northwest and 'NE' denotes northeast part of Baden-Württemberg State of Germany respectively with 80% confidence interval of Gaussian process and one of its realization (dashed line).

Figure 14 Copula distances of API time series in moving time window: moving covariance (top), moving correlation (second), distance type3 (third) and distance type4 (bottom)

Figure 15 Copula distance type3 (top) and type4 (bottom) between 4 discharge and 1 API time series which is aggregated for all the daily precipitations depicted in Figure 12

Figure 16 Copula asymmetry and copula distances for 30 simulated and one observed discharge time series at Plochingen between 1965 and 2000: minimum of asymmetry2 for the time lag $k=2$ [days] (top), copula distance type1 (middle), copula distance type2 (bottom)

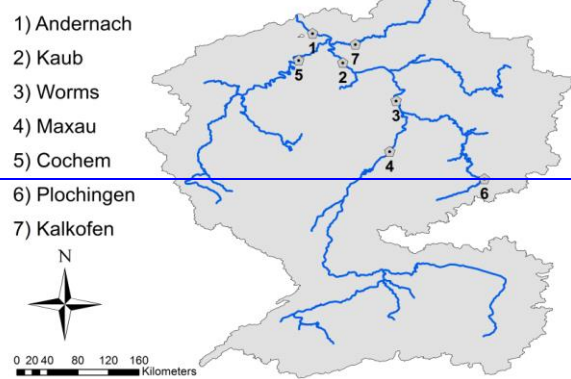
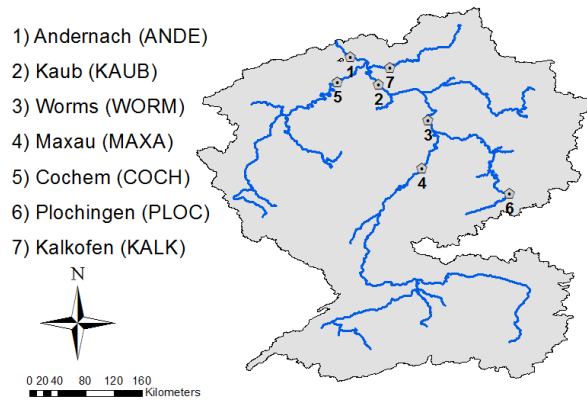


Figure 1. Locations of 7 discharge gauging stations in the Upper Rhine Region

Formatted: Font: Bold

Formatted: Font: Bold

Formatted: Font: Bold

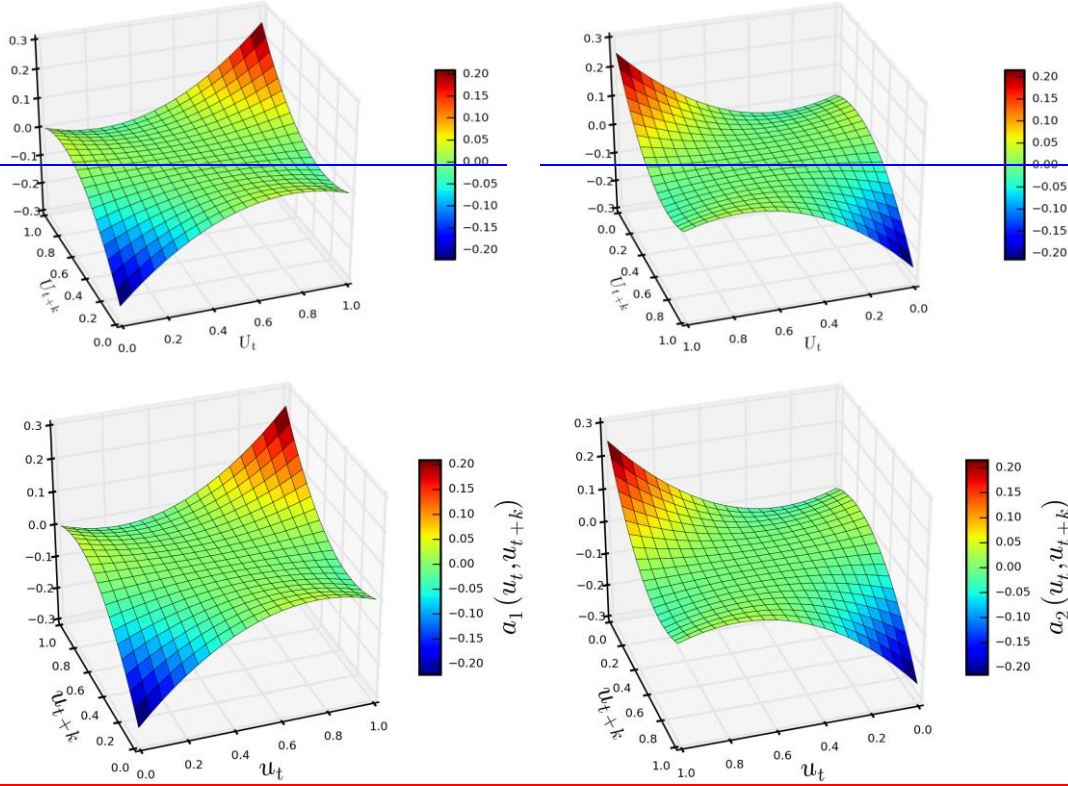


Figure 2. Visualization of the functions $a_1(u_t, u_{t+k}) = (u_t - 0.5)(u_{t+k} - 0.5)((u_t - 0.5) + (u_{t+k} - 0.5))$ (left) $(u_t - 0.5)(u_{t+k} - 0.5)((u_t - 0.5) - (u_{t+k} - 0.5))$ and $a_2(u_t, u_{t+k}) = (u_t - 0.5)(u_{t+k} - 0.5)((u_t - 0.5) - (u_{t+k} - 0.5))$ (right) which displays the contribution of single realization of (U_t, U_{t+k}) to asymmetry functions $A_1(k) = E[(U_t - 0.5)(U_{t+k} - 0.5)((U_t - 0.5) + (U_{t+k} - 0.5))]$ -asymmetry1 (left) and $A_2(k) = E[-(U_t - 0.5)(U_{t+k} - 0.5)((U_t - 0.5) - (U_{t+k} - 0.5))]$ asymmetry2 (right)

Formatted: Font: Bold
Formatted: Font: Bold
Formatted: Font: Bold
Formatted: Lowered by 8 pt

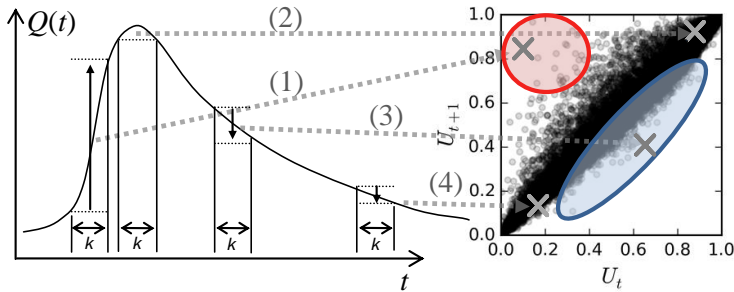


Figure 3. Sketch of the transformation of the values from sample hydrograph (left) to the points on scatterplot of ranks (right): empirical copula calculated from two values separated by time lag $k = 1$ ~~days~~ in a discharge time series of Andernach where rank correlation is 0.9870 ~~rank correlation = 0.9870~~ , $A_1(k=1) = -0.0002398$ and $A_2(k=1) = -0.00011037$. The possible combinations of high and low values, which has large impacts on asymmetry, are numbered: (1) low to high, (2) high to high, (3) high to low, (4) low to low. Negative contribution to A_2 asymmetry2 is drawn with red circle and positive contribution with blue oval.

Formatted: Font: Bold

Formatted: Font: Italic

Formatted: Lowered by 5 pt

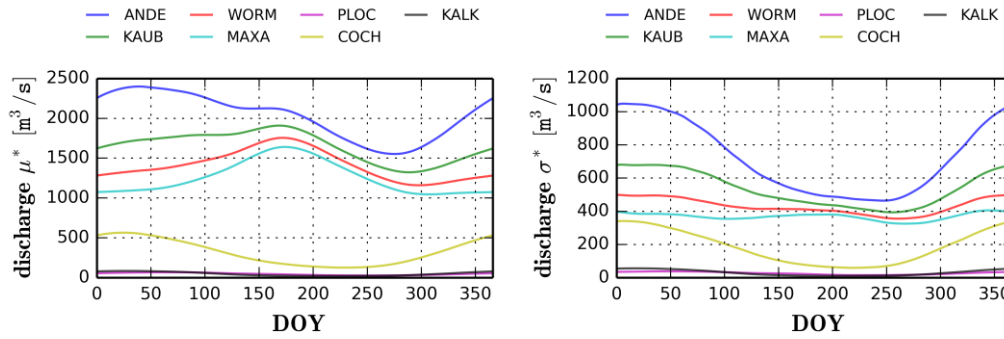


Figure 4. Annual cycles of mean discharge measured at seven sites in the Rhine basin after smoothing (left) and annual cycle of standard deviation after smoothing (right)

Formatted: Font: Bold

Formatted: Font: Bold

Formatted: Font: Bold

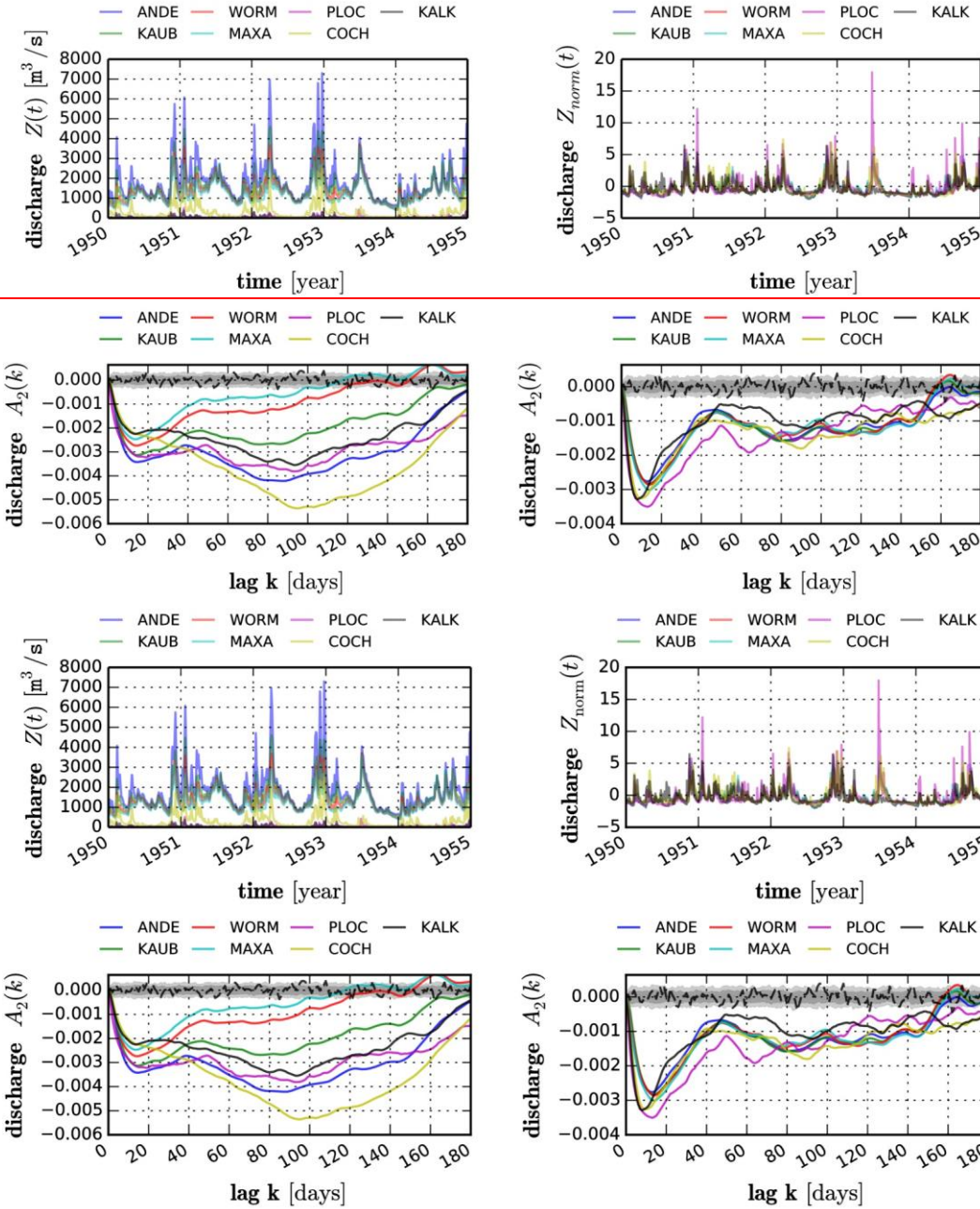


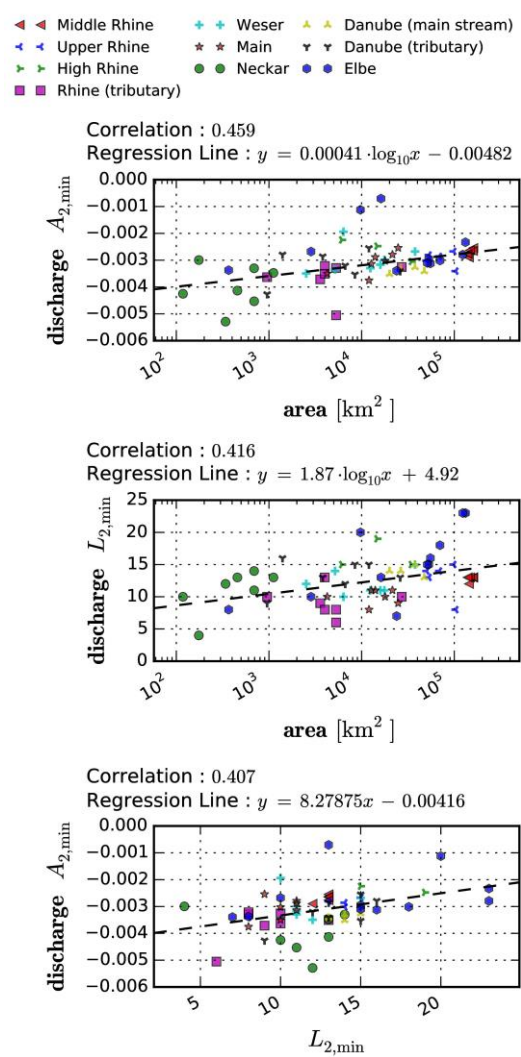
Figure 5. Discharge time series measured at seven sites in the Rhine basin between 1950 and 1955 before applying normalization (upper left) and after applying normalization (upper right). The variation of

Formatted: Font: Bold

Formatted: Font: Bold

Formatted: Font: Bold

731 $A_2(k)$ ~~asymmetry2 function~~ calculated for entire time series before applying normalization (bottom left)
 732 and after applying normalization (bottom right) with 90% confidence intervals (grey) calculated for 100
 733 realizations of Gaussian process (dashed line is $A_2(k)$ calculated for one of the realization of Gaussian
 734 process).



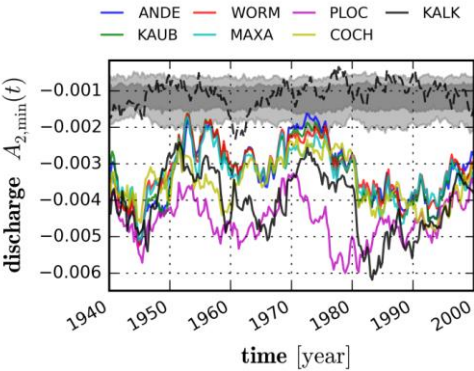
735 **Figure 6.** Relation between ~~a~~Asymmetry of discharge data and catchment characteristics: minimum of
 736 asymmetry2 $A_{2,min}$ of discharge and catchment area (top), ~~lag at minimum of asymmetry2~~ $A_{2,min}$ of
 737 asymmetry2 $A_{2,min}$ of discharge and $L_{2,min}$ (bottom)

Formatted: Font: Bold

Formatted: Font: Bold

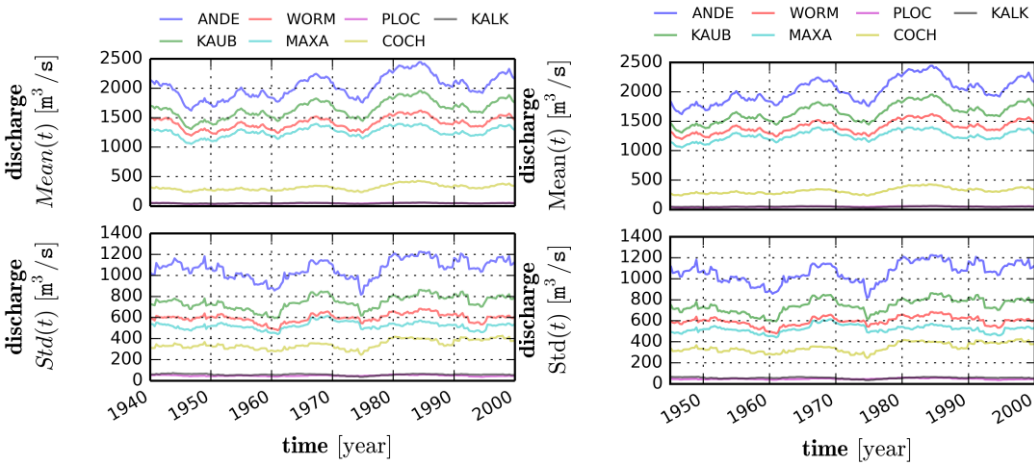
Formatted: Font: Bold

738 discharge and catchment area (middle), ~~minimum of asymmetry2~~ $A_{2,min}$ of discharge and ~~lag at~~
739 ~~minimum~~ $L_{2,min}$ of asymmetry2 of discharge (bottom)



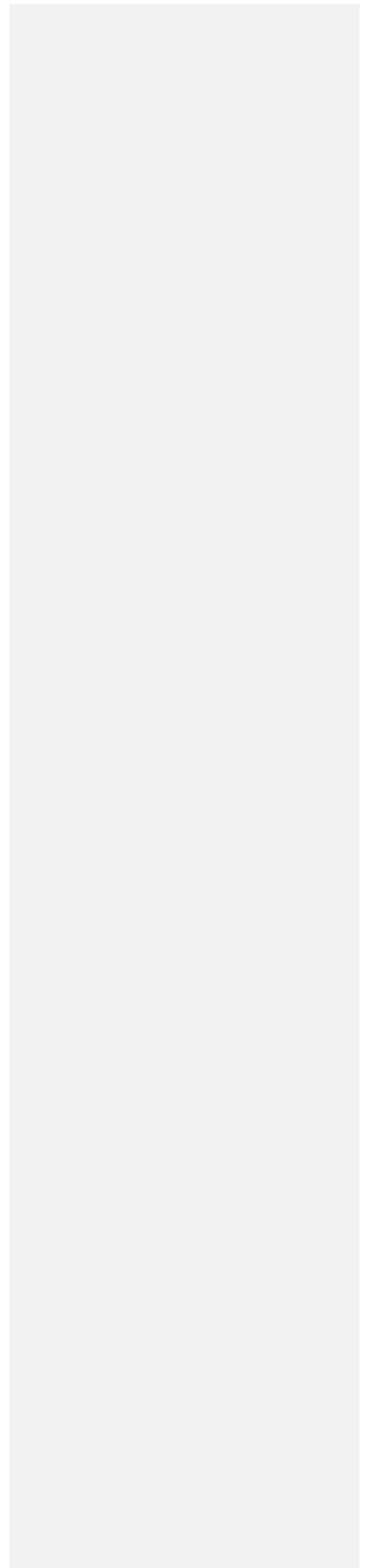
740
741 **Figure 7.** Temporal change of ~~minimum of~~ asymmetry2 : $A_{2,min}(t)$ for 7 discharge records and ~~for~~
742 ~~comparison~~ confidence intervals calculated from the Gaussian process (90% confidence interval with
743 grey color and 60% confidence interval with dark grey color) and one of its realizations (dashed line)

Formatted: Font: Bold
Formatted: Font: Bold
Formatted: Font: Bold

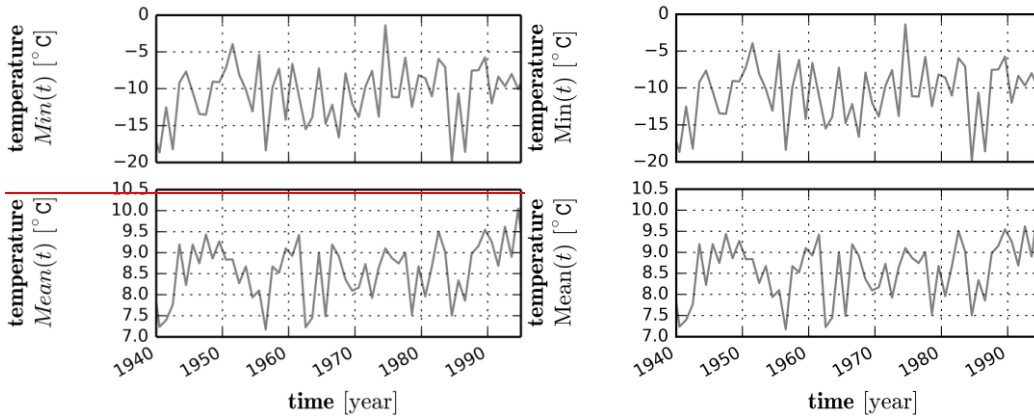


745
746 **Figure 8.** Moving average and standard deviation of the 7 daily discharge records for the window size $w =$
747 3000 (days)

Formatted: Font: Bold
Formatted: Font: Bold
Formatted: Font: Bold
Formatted: Font: Bold



750



751

752

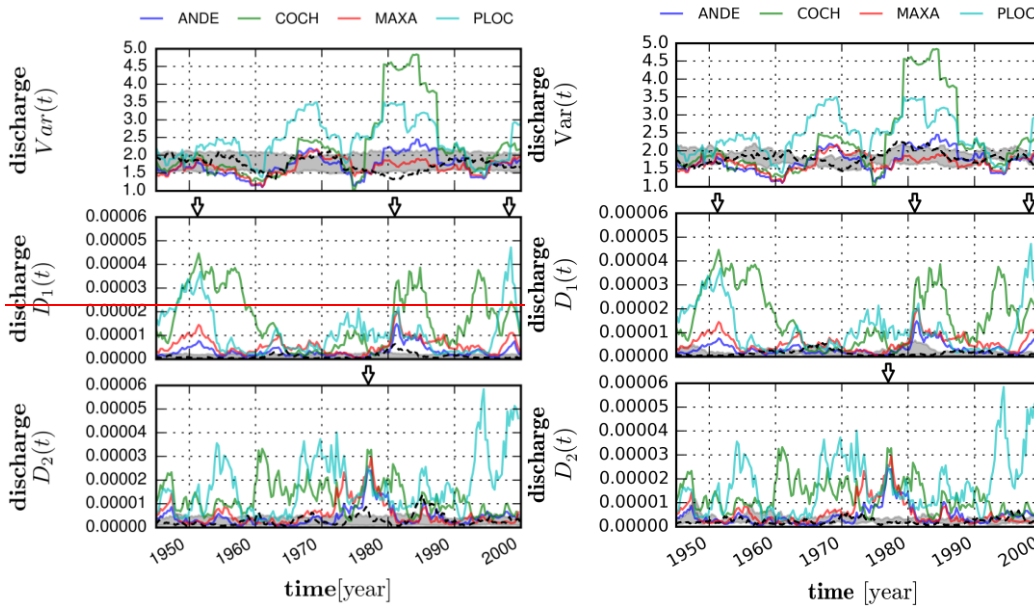
753

Figure 9. Annual minimum (upper panel) and mean of aggregated daily temperature (lower panel) in the Baden-Württemberg state of Germany

Formatted: Font: Bold

Formatted: Font: Bold

Formatted: Font: Bold



754

755

756

757

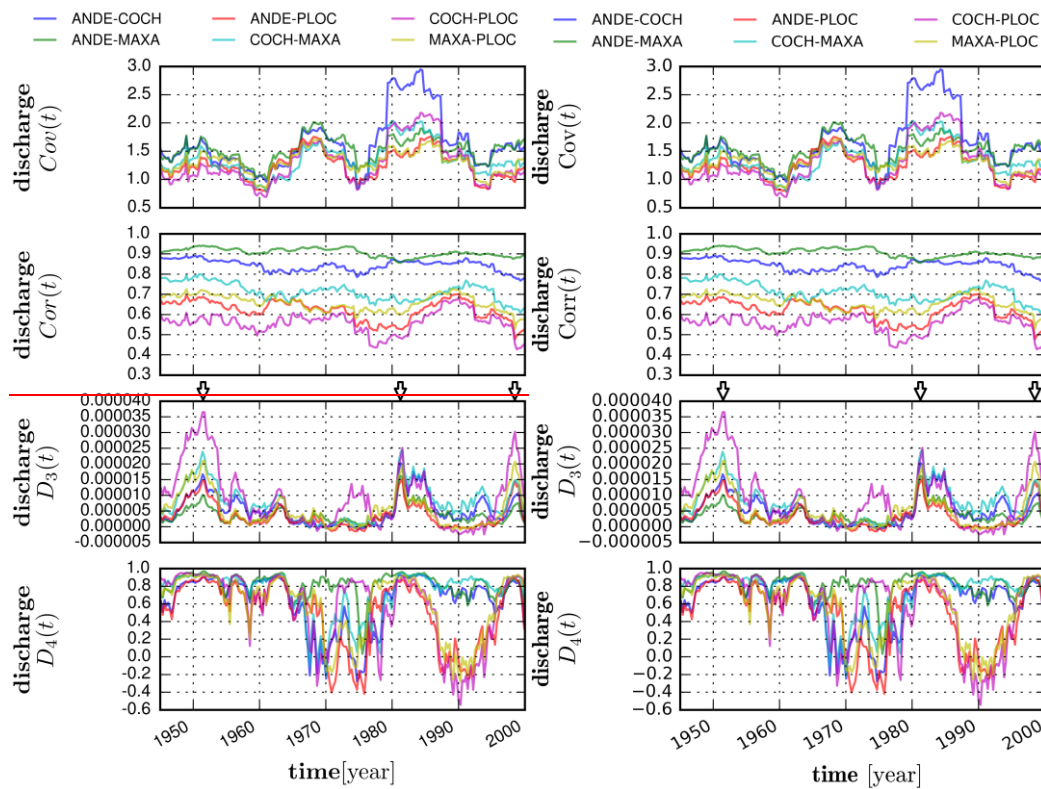
Figure 10. Copula distances of discharge time series in moving time window: moving-variance (top), distance type1 (middle) and distance type2 (bottom), each panel containing the with 80% confidence interval of Gaussian process and one of its realization (dashed line). The arrows point 1947, 1982, 2000

Formatted: Font: Bold

Formatted: Font: Bold

Formatted: Font: Bold

758 [and 1977 in which the clear signals of anomalies are detected for all four discharge time series:](#)
 759 [Andernach\(ANDE\), Cochem\(COCH\), Maxau\(MAXA\) and Plochingen\(PLOC\)\).](#)
 760



761
 762 **Figure 11.** Copula distances of discharge time series in moving time window: [moving](#) covariance (top),
 763 [moving](#) correlation (second), [copula](#) distance type3 (third) and [copula](#) distance type4 (bottom). [The arrows](#)
 764 [point 1947, 1982 and 2000 in which the clear signals of anomalies are detected for the comparisons](#)
 765 [between 4 discharge time series: Andernach\(ANDE\), Cochem\(COCH\), Maxau\(MAXA\),](#)
 766 [Plochingen\(PLOC\)](#)

Formatted: Font: Bold
 Formatted: Font: Bold
 Formatted: Font: Bold

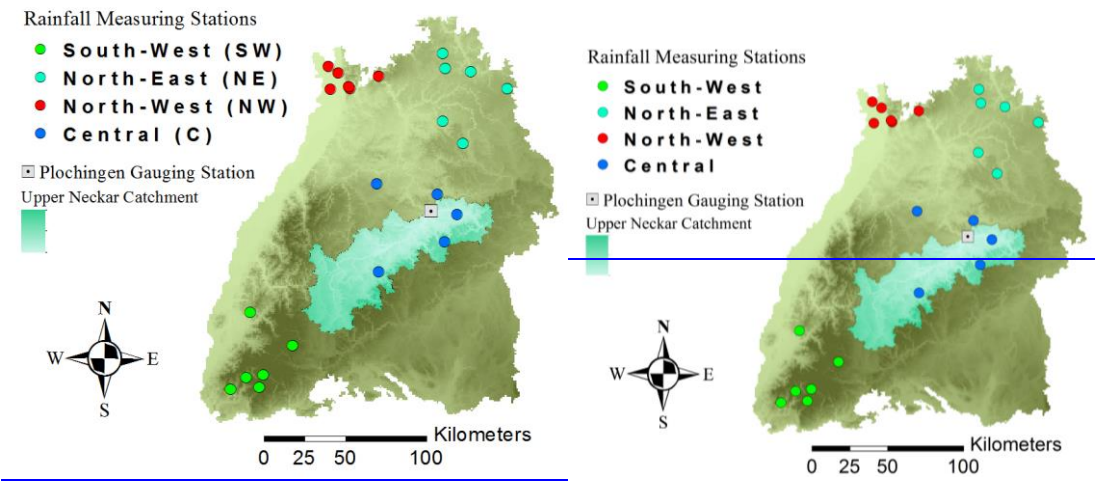


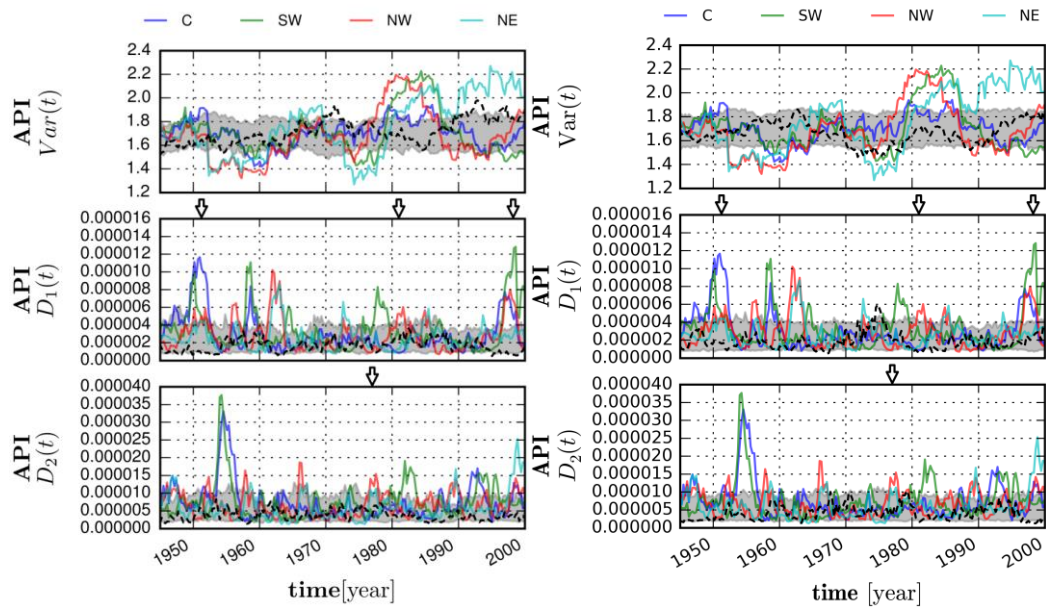
Figure 121212. Locations of the precipitation gauge stations within the Baden-Württemberg (Germany) indicated by coloured circles. Upper Neckar catchment is identified by the light drawn with green area and the location of the gauging station is indicated by drawn with a square

Formatted: Font: Bold

Formatted: Font: Bold

Formatted: Font: Bold

773



774

775 **Figure 13** Copula distances of API time series in moving time window: ~~moving~~ variance (top),
776 copula distance type1 (middle) and copula distance type2 (bottom) where ‘C’ denotes central, ‘SW’
777 denotes southwest, ‘NW’ denotes northwest and ‘NE’ denotes northeast part of [the](#) Baden-Württemberg
778 State of Germany, ~~each containing respectively with~~ 80% confidence interval of Gaussian process and one
779 of its realization (dashed line). [The arrows indicate the years in which anomalies are detected in the](#)
780 [previous analysis \(Fig. 10\)](#)

781

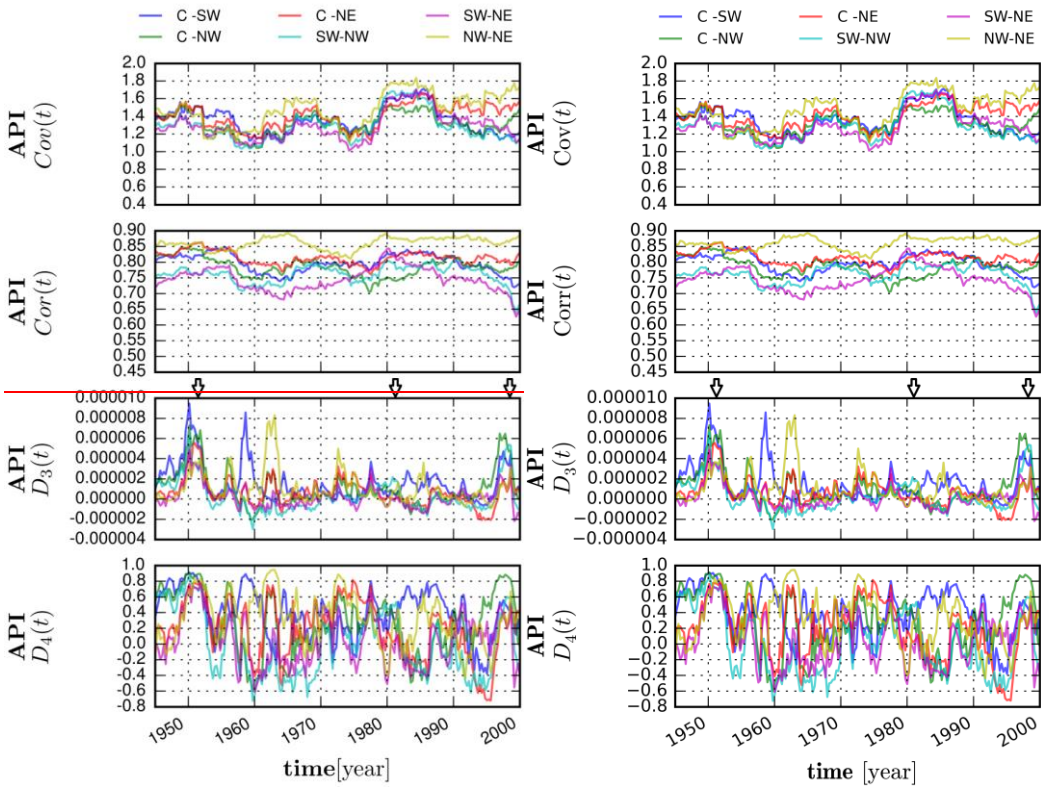
782

783

784

Formatted: Font: Bold
Formatted: Font: Bold
Formatted: Font: Bold

Field Code Changed
Formatted: Font: Not Bold
Formatted: Font: Not Bold



786

787 **Figure 14**, Copula distances of API time series in moving time window: **moving** covariance (top),
788 **moving** correlation (second), **copula** distance type3 (third) and **copula** distance type4 (bottom). **The arrows**
789 **indicate the years in which anomalies are detected in the previous analysis (Fig. 11 Fig. 14)**

790

791

Formatted: Font: Bold

Formatted: Font: Bold

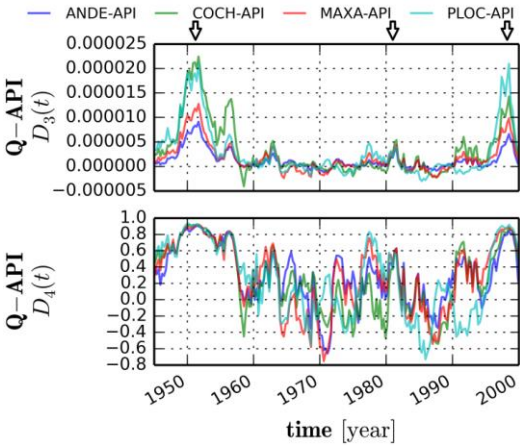
Formatted: Font: Bold

Field Code Changed

Formatted: Font: Not Bold

Formatted: Font: Not Bold

792



793

794

795

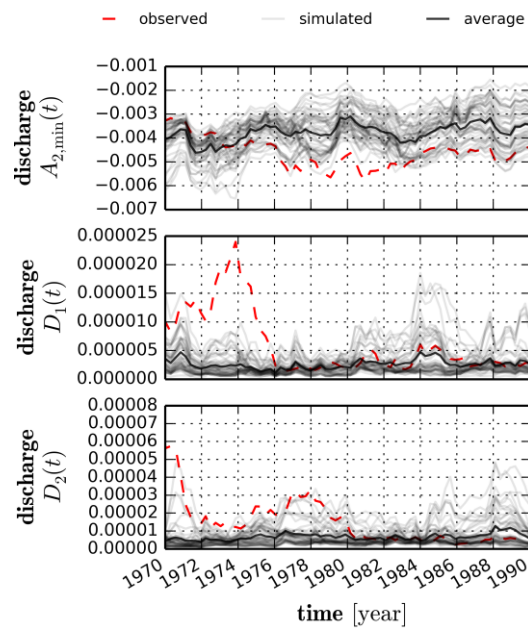
796

797

Figure 151515. Copula distance type3 (top) and type4 (bottom) between 4 discharge and 1 API time series which is aggregated for all the daily precipitations depicted in [Fig. 12](#)~~Fig. 12~~[Figure 12](#). The arrows indicate the years in which anomalies are detected in the previous analysis ([Fig. 11](#)~~Fig. 11~~[Fig. 11](#))

- Formatted:** Font: Bold
- Formatted:** Font: Bold
- Formatted:** Font: Bold
- Formatted:** Font: Not Bold, Check spelling and grammar
- Formatted:** Font: Not Bold, Check spelling and grammar
- Formatted:** Font: Not Bold
- Formatted:** Font: Not Bold

798



799

800

801

802

803

804

805

806

Figure 16. Copula asymmetry and copula distances for 30 simulated and one observed discharge time series at Plochingen between 1965 and 2000: minimum of asymmetry2 $A_{2,min}$ for the time lag $k = 2$ (days) (top), copula distance type1 (middle), copula distance type2 (bottom)

Formatted: Font: Bold

Formatted: Font: Bold

Formatted: Font: Bold